

PETER A. SHARY (\*), LARISA S. SHARAYA (\*\*) & ANDREY V. MITUSOV (\*\*\*)

## THE PROBLEM OF SCALE-SPECIFIC AND SCALE-FREE APPROACHES IN GEOMORPHOMETRY

**ABSTRACT:** SHARY P.A., SHARAYA L.S. & MITUSOV A.V., *The problem of scale-specific and scale-free approaches in geomorphometry*. (IT ISSN 1724-4757, 2005).

An extended system of 18 basic land surface attributes, or morphometric variables (MVs), is presented, together with formulae and computation algorithms. MVs and related methods, including those relevant to oil spills and natural hazards, are described. All MVs, both discovered and not, are classified into six non-overlapping classes, with the general properties of each class elucidated. The problem of MV precision is studied on the basis of the concept that MVs are scale-free if tended to some finite limit as grid mesh approaches to zero (with enlarging map scale), and they are scale-specific in the opposite case. MV plots against grid mesh are studied experimentally. Due to roughness in natural landscapes, some scale-specific land form types, such as those of Gaussian or Troeh's classifications, occupy predicted areas for any terrain, as described by Shary's statistical hypothesis [Shary, 1995]. This is validated experimentally for 17 terrains. The Evans' phenomenon [Evans, 1980] is explained as a consequence of natural landscape roughness. Some natural terrain-specific deviations from values predicted by MV methods are described. An example of scale-free land form classification is presented, in which some terrain-specific hydrologically important geomorphologic features are described directly. A new concept of distribution areas for studying hydrological phenomena generalizes the concept of flow-lines for the case of the real (non-smooth) land surface, and is applied to oil spills. Future prospects and forthcoming trends in geomorphometry are discussed.

**KEY WORDS:** Geomorphometry, Digital Elevation Model, Scale, Geological structure, Land form classification, Oil spill.

### INTRODUCTION

The land surface plays an important role in studying numerous natural phenomena. It is able to reflect geological processes and phenomena being used in decoding of

lineaments, ring structures, etc., because the land surface itself creates conditions for these features to be expressed. It influences surface water movement and spatial variability of thermal regime of slopes. Land surface characteristics are numerous, here we outline the following five major ones (Shary & alii, 2002b):

- surface runoff,
- terrain dissection,
- geometrical forms,
- thermal regime of slopes,
- altitude zonality.

We encounter a somewhat unusual situation in the description of land surfaces. There are no such land surface attributes as slope gradient or aspect in the differential geometry of surfaces, because these characteristics deal with invariants of surface rotation as a whole, such as mean curvature (Young, 1805), while gradient essentially changes after such rotation. In other words, these land surface attributes (that we term morphometric variables, MVs) describe the system «land surface + gravitational field». Another example is a description of the system «land surface + solar irradiation field» using insolation. Generalizing these facts, we may say that the subject of geomorphometry is a mathematically double system, «land surface + vector field» (Shary, 1995), that is not sufficiently studied in mathematics (Koenderink & van Doorn, 1994).

Besides this, the land surface cannot be considered as smooth in many cases without contradicting observation. Richardson (see Mandelbrot, 1967) has shown in his study of the length of the coast of Britain at different scales that this length should be considered as infinite as the scale increases. On the other hand, such a line must have a limit length for a smooth surface (Sard, 1942). A strong dependence of some topographic attributes on scale (Evans, 1975; Shary & alii, 2002a) that makes comparisons of results obtained at different scales difficult, the absence of limit values at large scales, and statistical predictability of areas in any terrain occupied by certain land forms (Shary, 1995) are

(\*) *Institute of Physical, Chemical and Biological problems of soil science RAS, 142290 Pouchchino, Moscow region, Russia.*

(\*\*) *Institute of Volga Basin Ecology RAS, 445003 Tolyatti, Kamzina street 10, Kuibyshev region, Russia.*

(\*\*\*) *University of Hohenheim, Institute of Soil Science and Land Evaluation, D-70599, Stuttgart, Germany.*

other important phenomena that contradict the smooth land surface model, so that the latter may be regarded as non-adequate to corresponding purposes of land surface analysis. A belief even appears sometimes that, when land surface analysis is used, each phenomenon may be described only by its own scale (e.g., Klemeš, 1983; Phillips, 1988).

The purpose of this paper is to describe the current state of basic quantitative methods of geomorphometry, and to study the question of the precision of various MVs including together with their formulae and algorithms for their calculation. We will also discuss land form classifications, some general aspects of their relations to natural processes and phenomena, how to take into account the non-smooth nature of the land surface, and some other topics that refer to the use of geomorphometry in Earth sciences. The description of these questions is restricted to basic topographic attributes (i.e., by so-called general geomorphometry (Evans, 1972)). Numerous combinations or versions of topographic attributes are hardly considered herein; some examples are given, for example, by Wilson & Gallant (2000).

All calculations in this paper were carried out using Analytical GIS Eco (Shary, 2001).

## CLASSES OF MORPHOMETRIC VARIABLES

Clearly, it is impossible to describe even the major aspects of land surface actions listed in the Introduction by use of two or three MVs; conversely, the use of a large number of MVs would make operating considerably difficult without introducing of corresponding classification of these variables and underlying concepts, such as those of land form types. This section describes the necessary classification onto six non-overlapping classes of MVs and land forms.

It is desirable to start from definitions. A morphometric variable (MV) is a quantitative land surface attribute that is defined in each map point. MVs are a particular case of morphometric characteristics that may refer in the general case not to a definite point, but to an area or a line on a map, like, for example, depression volume, length of a curve, or average value of some MV for a given terrain.

MVs may describe a fixed vicinity of a given point (local MVs) or need consideration of extended land surface portions, which size depends on terrain specifics and cannot be defined in advance (regional MVs); besides this, some MVs may need for their definitions to test all closed planetary surface (global, or planetary MVs). Further, MVs may describe the system «land surface + vector field» (field-specific MVs), or refer only to the description of the surface itself ignoring any vector fields (field-invariant MVs). The same refers to land forms. This gives a classification that is presented in table 1.

TABLE 1 - Classes of morphometric variables and concepts (Shary & alii, 2002a)

<i>Morphometric variables and land forms</i>	<i>Local</i>	<i>Regional</i>	<i>Global</i>
Field-specific	Class A	Class B	Class B'
Field-invariant	Class C	Class D	Class D'

Local MVs (such as gradient) are calculated at a given point of an elevation matrix using fixed filters, while regional MVs need to use «searching» filters, the size of which is determined by terrain specifics during calculations. For example, to calculate depression depth at a given point (a regional MV), one needs to detect this depression, an operation that needs a searching filter, fig. 1.

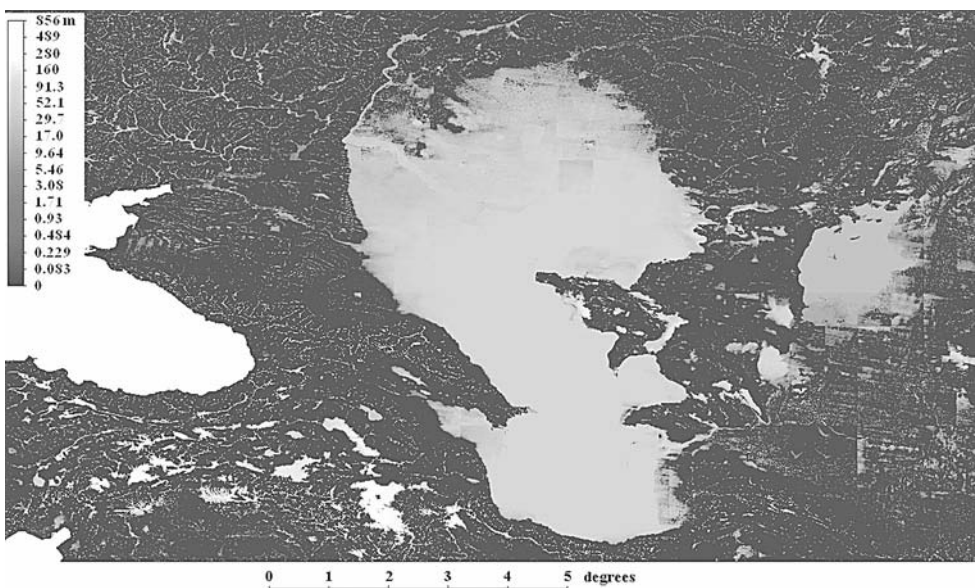


FIG. 1 - Map image of depression depths for Aral-Caspian region. Bottoms of Aral and Caspian seas were replaced by their free water surface. Grid mesh 2.7 km, GTOPO30 data, latitude/longitude coordinates. Maximal depth of Caspian depression is 170 m (average depth 47.6 m), that of Aral depression is 39 m (average 16.0 m), boundaries are at altitudes of 31 and 60 m, respectively.

Currently MVs are known in classes A, B, and C; MVs of other classes (i.e., D, B', D') are not discovered yet. Spherical (also Fourier, etc.) harmonics as such do not give physically meaningful morphometric variables. They only serve to represent altitude data.

## TWO ACCUMULATION MECHANISMS

Surface runoff of dry and liquid materials is one of most important "topography actions" related to such phenomena as denudation, erosion, and surface water hydrology. It is important to distinguish two accumulation mechanisms due to surface runoff specific features in plan and in profile, fig. 2.

It was proven (Shary, 1995, theorem 4) that plan curvature is a quantitative measure of a flow-line divergence. Therefore, the plan curvature  $k_p$  characterizes the first accumulation mechanism at a local level. Shary & Stepanov (1991) and Mitasova & Hofierka (1993) independently argued that horizontal (or tangential) curvature  $k_b$  as in-

roduced by Krcho (1983) better describes the first accumulation mechanism. It was proven also (Shary, 1995, theorem 5, see also Shary & alii, 2002a) that the second accumulation mechanism is described at a local level by vertical (or profile) curvature  $k_v$ .

Aandahl (1948) has shown qualitatively that  $k_b$  and  $k_v$  locally describe spurs and terraces, correspondingly. By this definition negative  $k_b$  refer to concave spurs, whereas positive  $k_b$  corresponds to convex ones; negative  $k_v$  refers to concave terraces, while positive  $k_v$  refers to convex ones. Maps of these spurs and terraces are shown in fig. 3.

Sometimes errors appear in maps of vertical curvature due to widely spaced contour lines (when elevation is digitized from topographic maps), but this was not the case in Danki forest terrain shown in fig. 3, because of detailed topographic map and relatively high slope steepness (average  $2.2^\circ$ ) of the terrain. This was confirmed also by field observations, and by essential soil and vegetation changes observed near the wide concave terrace (Shary & alii, 2002b).

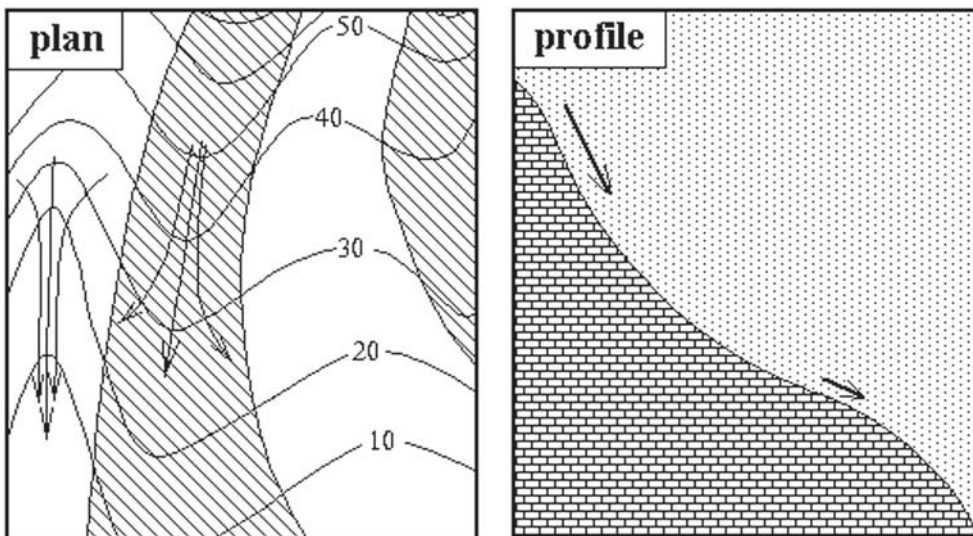
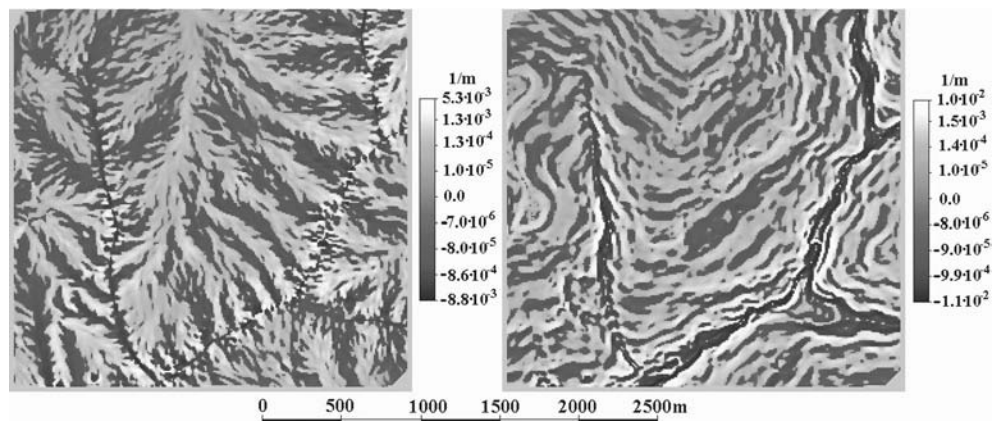


FIG. 2 - Two accumulation mechanisms. Left - the first one (flow-line convergence in plan), right - the second one (relative flow deceleration on concave in profile slopes). Downslope directed flow-lines are perpendicular to contour lines (curves with numbers), they are shown as curves with arrows.

FIG. 3 - Map images of Aandahl's spurs (left) and terraces (right) for the same terrain calculated using elevation matrix with grid mesh 10 m. These land form types refer to the two accumulation mechanisms described at a local level. Concave spurs ("hollows") and concave terraces are shown by dark colors, convex spurs and terraces are shown by light colors.



In an attempt to classify soil drainage status using topography, Troeh (1964) has suggested land form classification based on the signs of  $kh$  and  $kv$ , fig. 4.

Local MVs are based on differentiation of elevation by plan coordinates, while calculation of regional MVs needs integration. To describe the first accumulation mechanism, catchment area (up-slope area),  $MCA$ , is used, fig. 5.

### THE PROBLEM OF PRECISION OF MORPHOMETRIC VARIABLES

Richardson (see Mandelbrot, 1967), in his study of the dependence of the Britain coast length on scale, has shown that this length infinitely increases as the detail of topographic maps grows. This result means that the land surface cannot be considered as differentiable (i.e., smooth) without contradicting observation. Indeed, in the case of a smooth land surface, its contour lines must be smooth, that is, they should have a finite length (Sard, 1942). The absence of the latter, consequently, implies the non-smooth nature of the land surface.

To explain this important item in more detail, we use an example of a liquid flow that arises from an oil spill that starts at a given point, fig. 6. During an oil spill, oil flows round each terrain hillock resulting in oil flow branching. Immediately below that hillock flow confluence is observed. Since there are numerous out-of-scale hillocks at any scale, the process is described in general by a model of multiple oil flow branching and confluences, that is, by a model of a non-smooth surface. So, the non-smooth nature of the land surface appears to be a result of the presence, at any scale, of out-of-scale surface non-uniformities, which are not characteristic of a smooth surface.

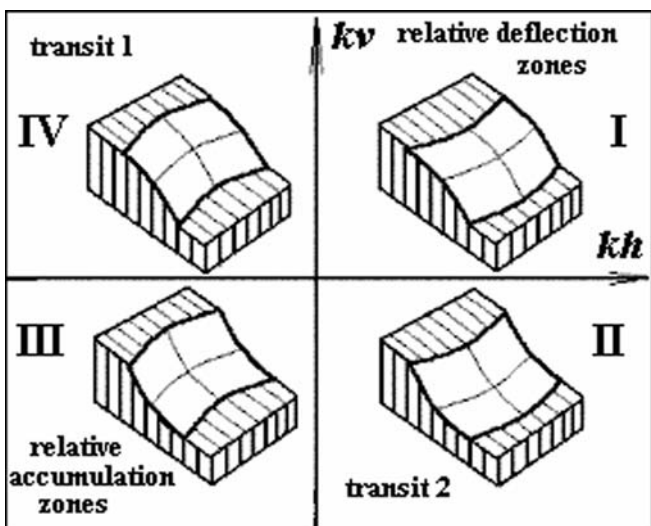


FIG. 4 - Troeh's land form classification by signs of horizontal ( $kh$ ) and vertical ( $kv$ ) curvatures.

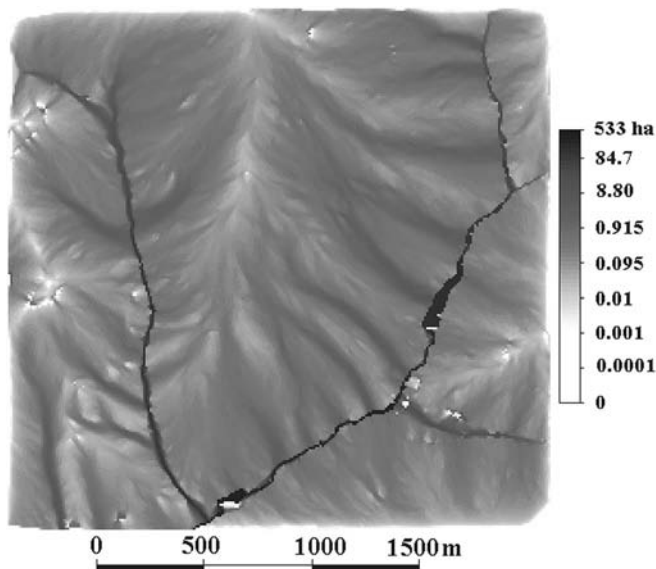


FIG. 5 - Map image of catchment area for the same terrain as in fig. 3. It shows both ephemeral drainage swales («potential» rivers) and perennial channels («realised» rivers) in the hydrological network.

On the other hand, the non-differentiable nature of the land surface means that there are no differential MVs in nature. In practice, we replace derivatives of elevation by finite differences, but the «cost» for this is a dependence of local MVs on grid mesh.

The dependence of MVs (mostly, of local ones) on grid mesh  $w$  results in the problem of the precision of MVs. Indeed, if differential MVs do not have limit values as  $w \rightarrow 0$ , there are no also precise values of these MVs, so that no precision may be defined for them. But how one may consider a quantitative science with no precision concept? This is the problem of precision in geomorphometry. This paper is devoted, in part, to its solution.

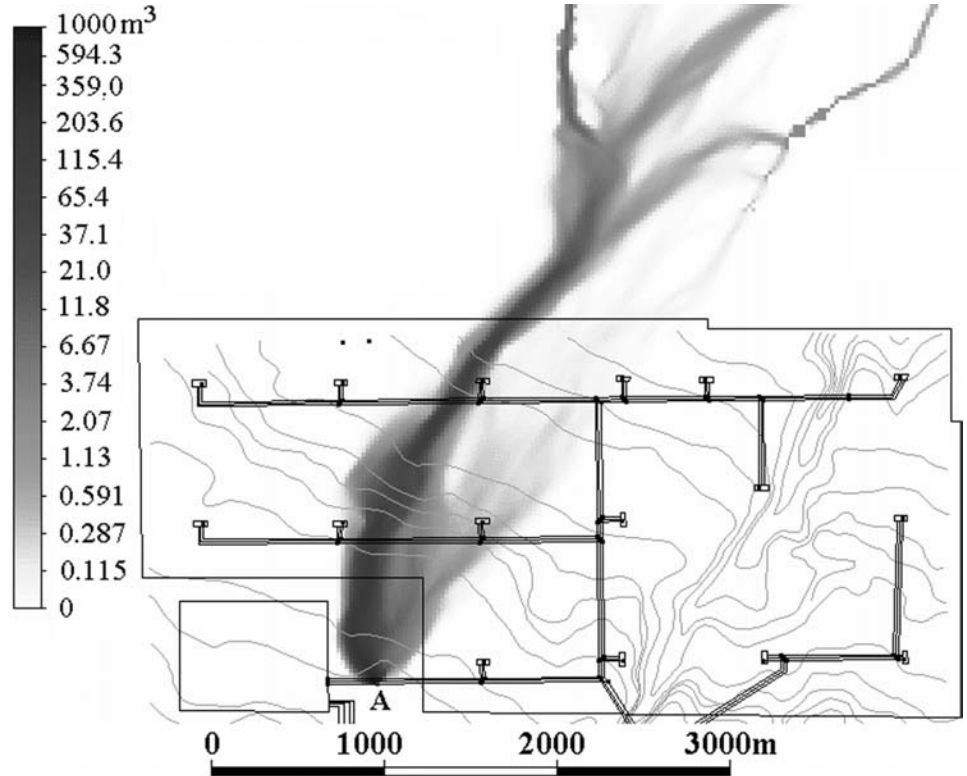
### THE SYSTEM OF MORPHOMETRIC VARIABLES

It is desirable before further discussion of the precision of MVs to make the reader more familiar with the modern system of basic MVs, including their formulae and algorithms, because this topic was not discussed in sufficient details in the geological literature, to our knowledge. Elevation is considered here as a source of initial data for calculation of other MVs and it can be determined with any desirable precision, as is common in the study of geodesy. For calculations, we assume the so-called topological restriction that consists in refusing to consider any sources of ambiguities in elevations (Shary, 1995).

#### Class A

The concept of gradient is commonly known, its module being slope steepness  $GA$ , and its direction being slope

FIG. 6 - Maximal distribution area from point A on a pipeline. The legend shows oil volume that passes through given map pixel. Curves are contour lines, straight lines are pipelines. Grid mesh is 8 m, Gauss-Krüger projection.



aspect  $A_0$ . Slope steepness units may be degrees ( $GA$ ), or be dimensionless as a tangent ( $G=\tan GA$ ) or a percentage ( $GP=100\cdot G$ ), essentially also dimensionless. The tangential force responsible for surface runoff is proportional not to gradient, but rather to the gradient factor  $GF$  that is equal to  $\sin GA$  (e.g., Strahler, 1952). Slope aspect  $A_0$  is usually calculated from the geographical North clockwise, ranging from 0 to 360°, although other definitions are possible, such as  $A_{90}$  (from 90°),  $A_{180}$  (from 180°) and so on. Slope aspect is the only anisotropic MV that effectively decodes lineaments and other geological structures, and its legend may be changed without re-calculation by a simple cyclic replacing of colors (e.g.,  $A_0$  to  $A_{90}$ ).

Decoding of a ring geological structure in the Crimea Penninslula using  $A_0$  is shown in fig. 7.

Formulae of  $GA$  and  $A_0$  are:

$$GA = \arctan(p^2 + q^2)^{1/2},$$

$$A_0 = -90[1 - \text{sign}(q)](1 - |\text{sign}(p)|) + 180[1 + \text{sign}(p)] - \frac{180}{\pi} \text{sign}(p) \arccos \frac{-q}{(p^2 + q^2)^{1/2}},$$

where

$$\text{sign}(x) = \begin{cases} 1 & \text{for } x > 0 \\ 0 & \text{for } x = 0 \\ -1 & \text{for } x < 0 \end{cases}$$

and

$$p = \frac{\partial z}{\partial x}, \quad q = \frac{\partial z}{\partial y}$$

are partial derivatives of elevation  $z$  by plan coordinates  $x$  and  $y$ . Aspect cannot be defined in special points, where  $GA=0$ .

Another MV of class A that depends on first derivatives is slope insolation  $F$ . This MV describes the system «land surface + solar irradiation» and therefore depends on two angles that define the current angular position of the Sun: azimuth  $a$  and angle from horizon  $b$ . Insolation is given by the formula

$$F(a, b) = \frac{50(1 + \text{sign}[\cos(90-a) - \sin(90-a)](p \sin b + q \cos b)) [\cos(90-a) - \sin(90-a)](p \sin b + q \cos b)}{(1 + p^2 + q^2)^{1/2}},$$

azimuth is in the range 0 to 360° (counted from the North clockwise), and the angle  $b$  varies from 0 to 90°. Insolation units are percentages of the value obtained for solar rays incident perpendicular to surface (this value is 100%);  $F$  changes from 0 to 100%. Local description means that hills may have a shady side, but do not produce shadows, because a shadow is a regional concept. It is not difficult to express insolation by slope steepness and aspect. Neglecting shadows, insolation is equal to:

$F(a, b) = 100 \cdot [\tan GA / (1 + \tan^2 GA)^{1/2}] \cdot [\sin b / \tan GA - \cos b \cdot \sin(a - A_0)]$ ; the interrelation of slope steepness and insolation is shown in fig. 8.

Now one may deduce formulae of boundary curves for points in fig. 8 from the last formula:

$$F(a, b) = 100 \cdot \sin b / (1 + \tan^2 GA)^{1/2} - 100 \cdot [\tan GA / (1 + \tan^2 GA)^{1/2}] \cdot \cos b, \\ F(a, b) = 100 \cdot \sin b / (1 + \tan^2 GA)^{1/2} + 100 \cdot [\tan GA / (1 + \tan^2 GA)^{1/2}] \cdot \cos b.$$

It follows from here for small  $GA$

$$F(a,b) \approx 100 \cdot \sin b \pm 100 \cdot \cos b \cdot \tan GA;$$

and it is seen now that the thermal regime of slopes is better described by slope insolation than by aspect. For example, for  $b=35^\circ$  and  $GA=2^\circ$  one obtains  $F=57.36 \pm 2.86\%$ , that is, deviations in insolation for any aspect do not exceed 5% of the value for horizontal surface (57.36%), while changes of aspect may be sufficiently large.

There are two first derivatives, so, only two functions of them ( $GA$ ,  $A_0$ , and  $F$ ) are independent; slope

steepness and insolation may be recommended for statistical comparisons between MVs and other landscape features.

Surface curvatures are described not only by Gaussian quadratic form coefficients (as in differential geometry of surfaces), but also by curvatures of normal sections naturally marked by a gravitational field on a surface, fig. 9.

Two of these directions,  $aa'$  (downslope) and  $bb'$  (along contour line), are marked by gravitational field, others – by the surface itself.

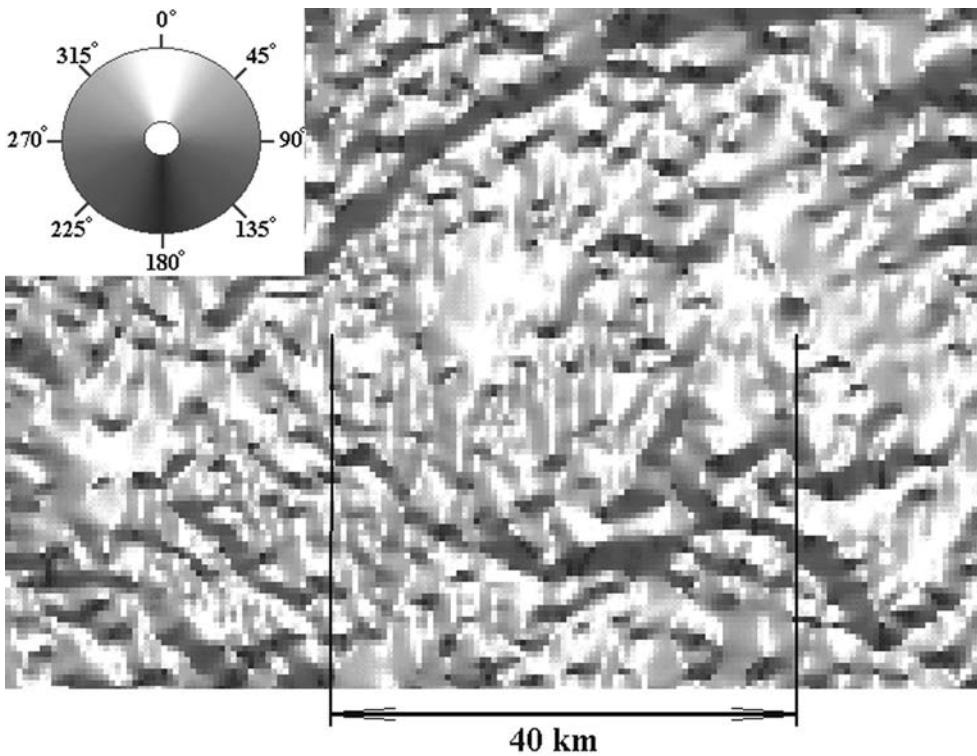


FIG. 7 - Interpreting a ring geologic structure in the Crimea Peninsula using slope aspect  $A_0$ . East and west slopes are not distinguished by colours. Grid mesh 500 m, Gauss-Krüger projection.

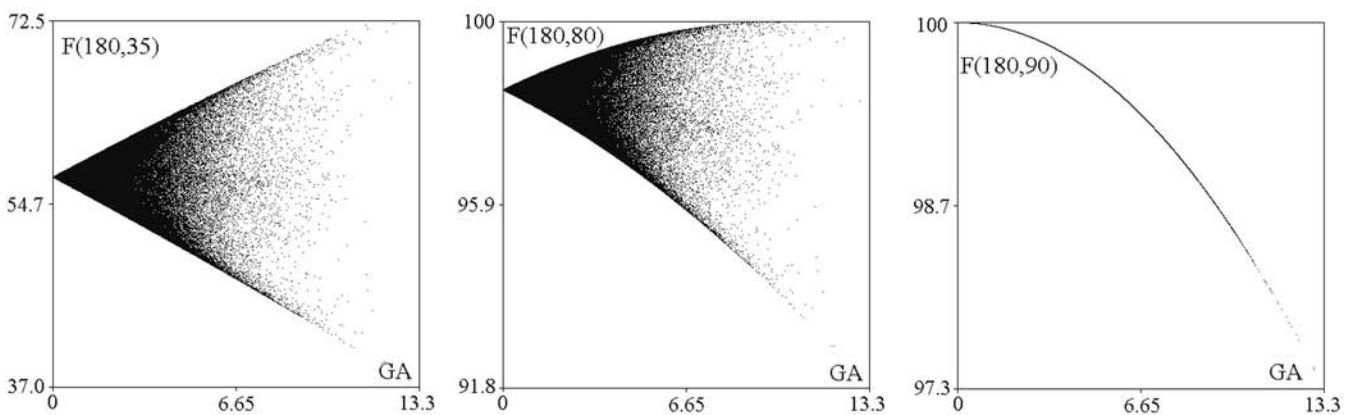


FIG. 8 - Plot of insolation  $F(a,b)$  against slope steepness  $GA$  at several values of the angle from horizon  $b$ . The terrain is the same as used in fig. 3. The upper and lower limiting curves apply to southern and northern slopes, respectively.

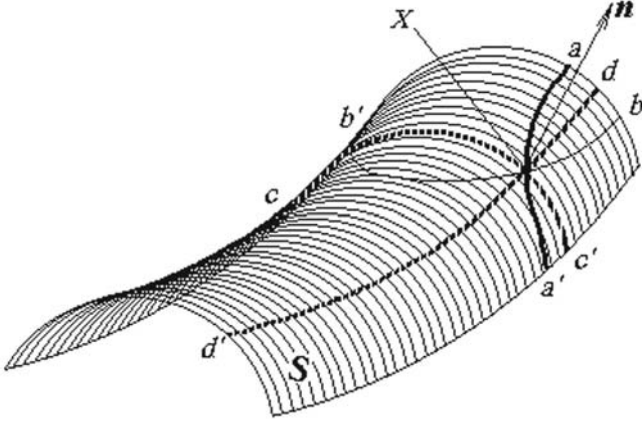


FIG. 9 - Four directions naturally marked on surface  $S$ .  $\mathbf{n}$  - normal to  $S$  at the point  $X$ ;  $aa'$  - flow-line;  $bb'$  - contour line;  $dd'$ ,  $cc'$  - main normal sections.

Curvatures of normal sections  $aa'$  and  $bb'$  are  $kv$  and  $kb$ , correspondingly (Shary, 1995). Their formulae are

$$kv = -\frac{p^2r + 2pqs + q^2t}{(p^2 + q^2)(1 + p^2 + q^2)^{3/2}}, \quad (1)$$

$$kb = -\frac{q^2r - 2pqs + p^2t}{(p^2 + q^2)(1 + p^2 + q^2)^{1/2}}, \quad (2)$$

where

$$p = \frac{\partial z}{\partial x}, \quad q = \frac{\partial z}{\partial y}, \quad r = \frac{\partial^2 z}{\partial x^2}, \quad s = \frac{\partial^2 z}{\partial x \partial y}, \quad t = \frac{\partial^2 z}{\partial y^2}$$

are partial derivatives of elevation  $z$  by plan coordinates  $x$  and  $y$ . Deduction of these formulae may be found in papers (Krcho, 1973; Young, 1978; Krcho, 1983; Pennock & alii, 1987).

Shary (1995) has suggested a system of 12 curvatures of classes A and C; the remaining curvatures of class A of his system are *rotor*

$$rot = \frac{(p^2 - q^2)s - pq(r - t)}{(p^2 + q^2)^{3/2}},$$

that describes flow-line curvature (positive when flow-lines rotate clockwise), and  $E$ , difference curvature

$$E = \frac{q^2r - 2pqs + p^2t}{(p^2 + q^2)(1 + p^2 + q^2)^{1/2}} - \frac{(1 + q^2)r - 2pqs + (1 + p^2)t}{2(1 + p^2 + q^2)^{3/2}}, \quad (3)$$

that describes the interrelationship of accumulation mechanisms (important also for land form classification). Using also unsphericity  $M$  (see next section), one may define formulae of horizontal excess curvature

$$kbe = M - E, \quad (4)$$

and  $kve$ , vertical excess curvature

$$kve = M + E; \quad (5)$$

their product is  $KR$ , total ring curvature

$$KR = \frac{[(p^2 - q^2)s - pq(r - t)]^2}{(p^2 + q^2)^2(1 + p^2 + q^2)^2}, \quad (6)$$

that describes terrain dissection and is proportional to  $rot^2$  (Shary & alii, 2002a).  $KA$ , total accumulation curvature (Shary, 1995; Shary et al., 2002a) is

$$KA = H^2 - E^2, \quad (7)$$

where  $H$  is mean curvature (see next section); it is a product  $kv \cdot kb$  and describes Troeh's land forms.

### Class C

In contrast to MVs of class A, MVs of class C are invariant with respect to any vector fields, that is, they formally ignore gravity. This provides an alternative land form description. We term land forms described by this method as geometrical forms (Shary & alii, 2002a).

Mean curvature (Young, 1806) results as an integral of curvature of normal section by angle of its rotation around normal vector  $\mathbf{n}$  (fig. 9) by  $360^\circ$ ; this gives the formula (Gauss, 1827)

$$H = -\frac{(1 + q^2)r - 2pqs + (1 + p^2)t}{2(1 + p^2 + q^2)^{3/2}}, \quad (8)$$

also  $H = 1/2(kv + kb) = 1/2(kmin + kmax)$  (Shary, 1995), where  $kmin$  and  $kmax$  are curvatures of main normal sections, that is, of curves  $dd'$  and  $cc'$  in fig. 9, respectively. It is known from the differential geometry of surfaces that  $H$  is zero for so-called minimal surfaces, for which surface area is minimal for a given contour.

Unsphericity is half of a difference between  $kmax$  and  $kmin$ ; its formula is (Shary & alii, 2002a)

$$M = \frac{\left\{ \left[ r \left( \frac{1+q^2}{1+p^2} \right)^{1/2} - t \left( \frac{1+p^2}{1+q^2} \right)^{1/2} \right]^2 (1+p^2+q^2) + \left[ pqr \left( \frac{1+q^2}{1+p^2} \right)^{1/2} - 2s \left( (1+q^2)(1+p^2) \right)^{1/2} + pqt \left( \frac{1+p^2}{1+q^2} \right)^{1/2} \right]^2 \right\}^{1/2}}{2(1+p^2+q^2)^{3/2}}, \quad (9)$$

this non-negative curvature is equal to zero on a sphere and positive outside a sphere, thus characterizing how far the surface is from a sphere. Minimal and maximal curvatures are expressed by  $M$  and  $H$  according to formulae (Shary, 1995)

$$kmin = H - M, \quad (10)$$

$$kmax = H + M. \quad (11)$$

Total Gaussian curvature  $K$  is product  $kmin \cdot kmax$ ; its formula is (Gauss, 1827)

$$K = \frac{rt - s^2}{(1 + p^2 + q^2)^2}, \quad (12)$$

A theorem was proven (Gauss, 1827) that any bending of surface that does not change lengths of curves on it, does not change total Gaussian curvature.

Only three of the curvatures (1) to (12) are independent; it was proven that  $H$ ,  $E$ , and  $M$  may be chosen as independent curvatures (Shary, 1995). Under this choice, other curvatures can be defined from these three, table 2.

TABLE 2 - Relation of other curvatures to the three independent ones,  $H$ ,  $E$ , and  $M$

Curvatures of units 1/m		Total curvatures (of units 1/m <sup>2</sup> )
$k_{max} = H+M$	$k_b = H-E$	$K = H^2-M^2$
$k_{min} = H-M$	$k_{ve} = M+E$	$KA = H^2-E^2$
$k_v = H+E$	$k_{be} = M-E$	$KR = M^2-E^2$

At the local level of description, land form is described by curvatures, not by gradient or aspect. Three algorithms for their calculation are currently considered as most popular: by Evans & Young (Evans, 1972; Young, 1978), by Shary (Shary, 1995), and by Zevenbergen & Thorne (1987). Comparison of these algorithms is given in Schmidt & alii (2003). These algorithms, however, often emphasize grid directions, preventing visual perception of map images. Therefore, Shary & alii (2002a) have suggested a modified Evans-Young algorithm for the curvatures, described here in the Appendix together with the original Evans-Young method.

An example of application of vertical curvature for forest boundaries decoding using a Shuttle Radar Topography Mission (SRTM) elevation matrix is shown in fig. 10. SRTM matrices are «raw» (i.e., not verified using ground measurements), in part, elevations are increased in forests by 3-6 meters, providing a possibility to decode forests and/or tree boundaries of agricultural fields in gently sloping terrains.

### Class B

Regional MVs of this class cannot be described by formulae, because they need integration over space to be used for calculation at given point. A known example of MV of this class is catchment area  $MCA$ , an integro-differential MV that describes up-slope area from which water could be collected to given pixel (Speight, 1968). An algorithm of  $MCA$  calculation is described by Martz & de Jong (1988), and corrected for taking into account multiple flow-line branching and confluence by Freeman (1991).

The hydrological meaning of this MV is as follows. During a stationary spatially uniform rainfall, when infiltration and evaporation are negligible,  $MCA$  describes surface water discharge in each given pixel, not in units of quantity of water (e.g.,  $\text{kg}\cdot\text{m}^{-2}\cdot\text{c}^{-1}$ ), but rather in units of area, to which that water falls during the same temporary interval. It is assumed also that all depressions are filled,  $MCA$  being constant inside each depression.

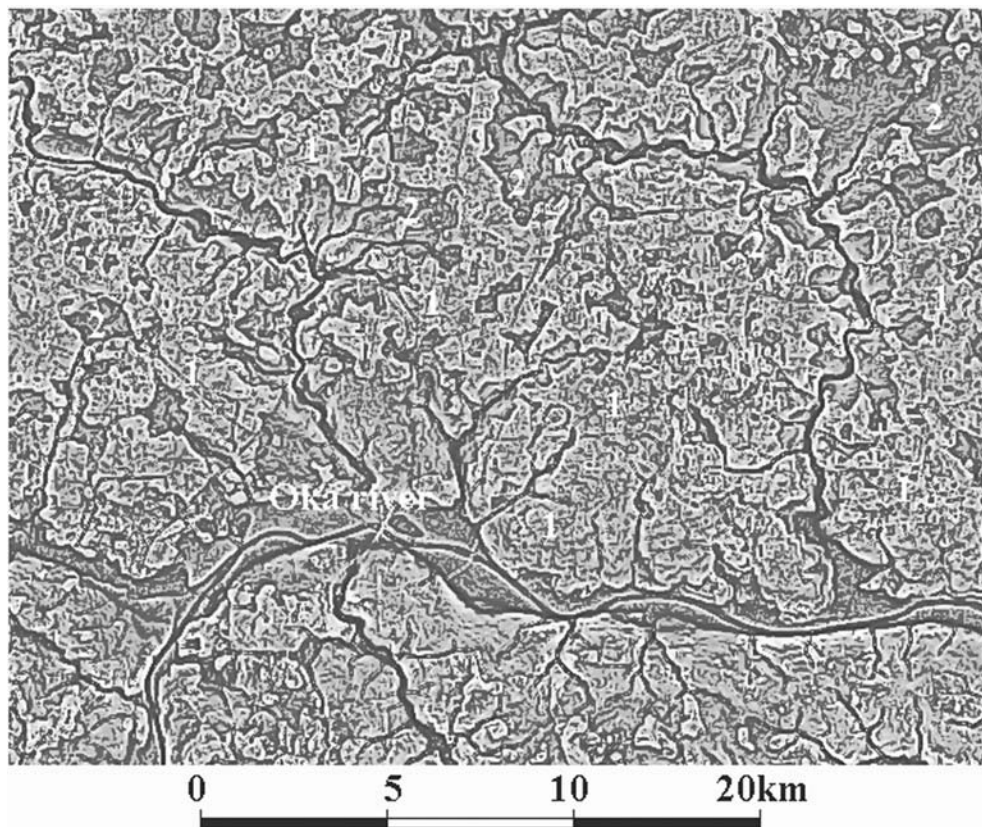


FIG. 10 - Use of vertical curvature to decode forest boundaries using SRTM grids of 90-m resolution (southern part of Moscow region, Russia). 1 - forest, 2 - absence of trees. Grid mesh is 100 m, Gauss-Krüger projection.

Mark (1979) has supposed that a critical area,  $MCA_{CR}$ , does exist, starting from which in each place where  $MCA$  exceeds  $MCA_{CR}$  permanent surface water is present in humid regions. Our results show  $MCA_{CR}$  is about 25 km<sup>2</sup> for the Moscow region (Russia), with annual precipitation 560 mm.

A comparison of  $MCA$  and rivers for the Spielweg region (Germany) is shown in fig. 11.

Catchment area plays an important role in the description of both potential (dry rivers) and realized (rivers, lakes) hydrological network (Speight, 1968,1974; Beven & Kirkby, 1979; Beven & Wood, 1983; Beven, 1987; Jenson & Domingue, 1988), soil properties (Martz & de Jong, 1990), erosion processes (Mitasova & alii, 1996, 1997; Mitas & alii, 1996, 1997; Mitas & Mitasova, 1998; Flanagan & alii, 2000). It is correlated with soil water saturation and vegetation distribution (Wigmosta & alii, 1994; Ryan & alii, 2000), and damage from rainfalls (Costa-Cabral & Burges, 1994), some parameters of road damage (Rafaelli & alii, 2001), and slope instability (Montgomery, 1994), and conditions of rivers beginning (Mark, 1979). The latter means that there is a critical value of  $MCA$  in humid regions, starting from which surface water appears in a form of permanent rivers and reservoirs. It is used in hydrological modeling (Beven & Kirkby, 1979; Rodhe & alii, 1996) and modeling of soil water saturation (Rafaelli & alii, 2001).

During calculation of  $MCA$ , depression depths are usually calculated also (Martz & de Jong, 1988) and these may play important role in geology description of some regions. Depths of Aral and Caspian depressions are shown in fig. 1. An arc-like pattern of depression in the Karakum desert shown in fig. 12 might appear an indication to non-eolian origin of this structure. Depression depth is an integral MV.

MacKenzie & Ryan (1999) noted that matrix inversion (i.e., replacing elevation  $Z$  by  $-Z$ ) before calculation results in replacing catchment area by dispersive area (Speight, 1974); depression depths are replaced in this case by hill

heights, at one of hill definitions known as B-hills (Shary & alii, 2002a). Hill heights of Europe (i.e., mountains, etc.) are shown in fig. 13.

Catchment area is constructed by «elementary» inputs from each pixel into a total map. Special weights might be applied to these inputs, or input from a single pixel may be considered thus making  $MCA$  more flexible. An example of a single-pixel input is maximal distribution area that describes placing liquid into a single point and takes multiple flow-line branching and confluence into account (fig. 6). Real distribution area is always inside a maximal one, and takes liquid infiltration into account, that is, it requires process modeling. Potentially, this approach provides an opportunity to restore liquid quantity using land surface, observed distribution area, and soil properties; this is important, for example, in oil spills.

## SOLUTIONS TO THE QUESTION OF PRECISION

For a long time, the question of absolute precision of MVs (not at a given scale) was avoided in the literature, at least in journals. In the first place, this was because of use of mostly local MVs which are differential and therefore have no limit values as grid mesh  $w \rightarrow 0$  for non-smooth land surface. However, Shary & alii (2002a) argued that regional MVs may have such limit values. We consider this question in more detail.

In calculating some MV, one may change grid mesh, thus in fact changing map scale. If one chooses several points on map with approximately equal slope steepness  $GA$ , the result may look like in fig. 14.

This example shows that slope steepness at a point may change two times if grid mesh changes 2 times. Evans (1975) calculated plots of dependence of average slope steepness  $GA$  on grid mesh; similar results are shown in fig. 15.

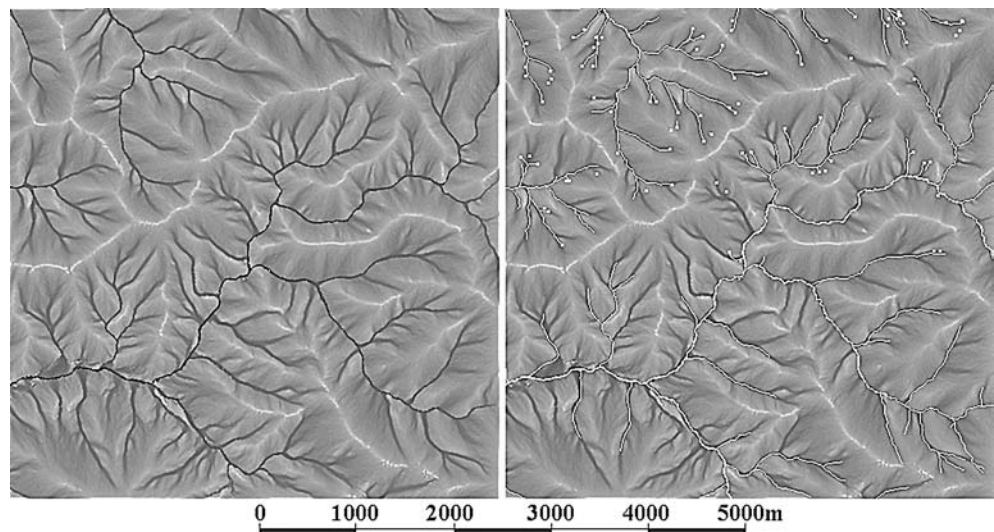


FIG. 11 - Map image of  $MCA$  (left) and rivers shown above it (right). Grid mesh 8 m, Gauss-Krüger projection.

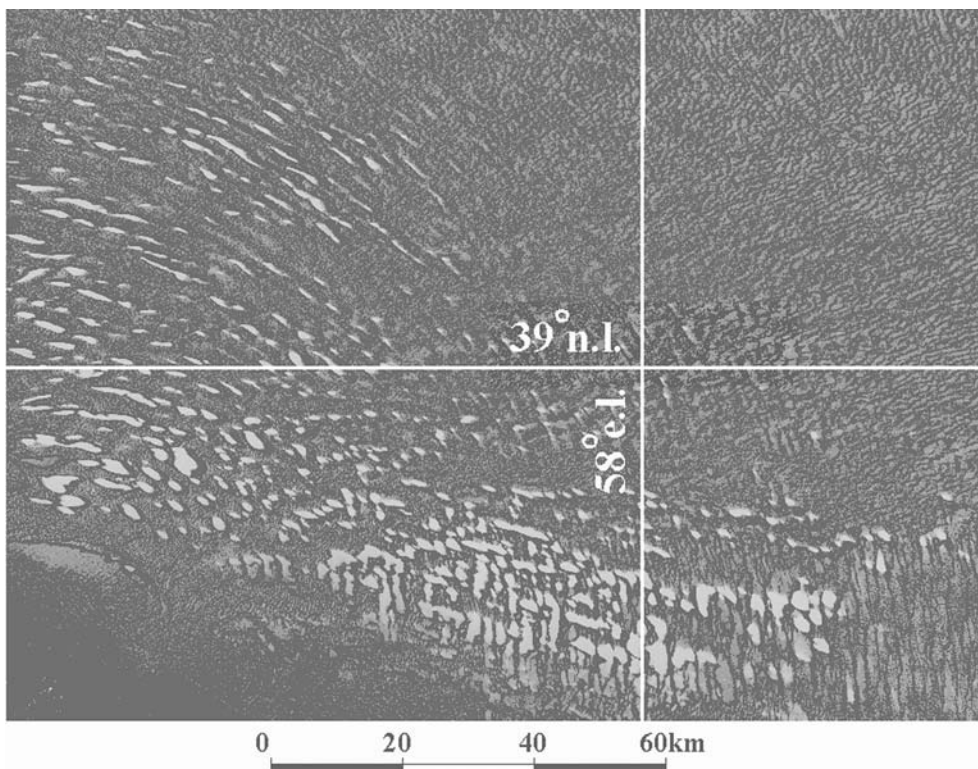


FIG. 12 - Depression depths (lighter-greater) in the south of Karakum desert. SRTM data, grid mesh 180 m, equal-area Behrgman's projection.

The model surface in fig. 15 (the curve «Noise-50») was obtained by adding pseudo-random numbers to a horizontal plane. This model surface is justified in the following way. If elevation does not depend on coordinate  $y$  in plan, when determined at grid mesh  $w$  slope steepness is  $\Delta z_i/w$ , where  $\Delta z_i$  is corresponding change in elevation at

the  $i$ -th matrix element. The matrix average steepness value is  $Z/w$ , where  $Z$  is average of  $\Delta z_i$ . Since trend of this quasi-stochastic, «noisy» surface is a horizontal plane, all  $\Delta z_i$  may have a single order of value, and  $Z$  may not depend on  $w$ . When slope steepness is proportional to  $1/w$ , that is, infinitely grows as  $w$  diminishes, and tend to zero

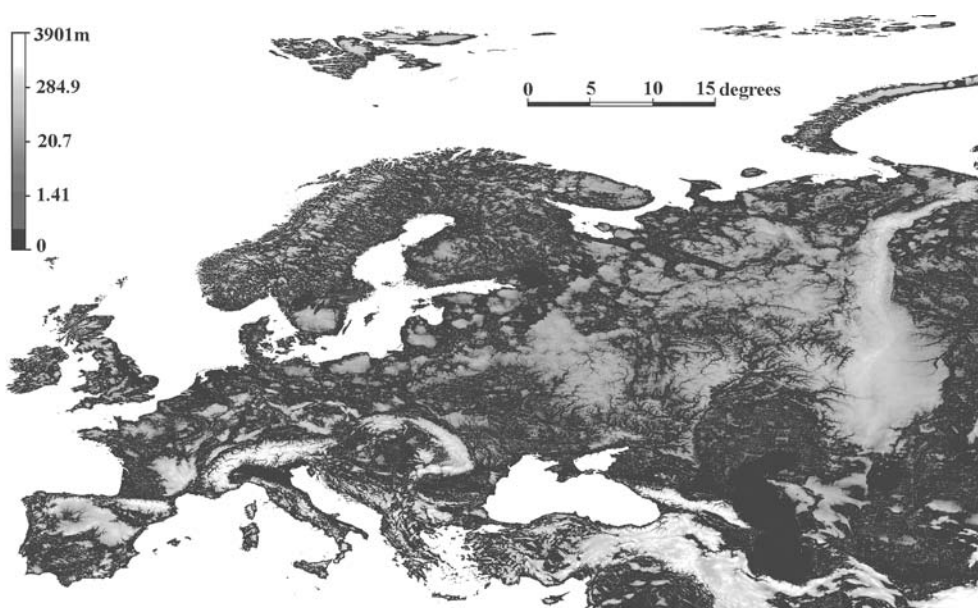


FIG. 13 - Map image of B-hill heights (lighter-greater) of Europe. GTOPO30 data, grid mesh 4.5 km, Cartesian coordinates latitude-longitude. Volume, area and other characteristics of each B-hill can be computed.

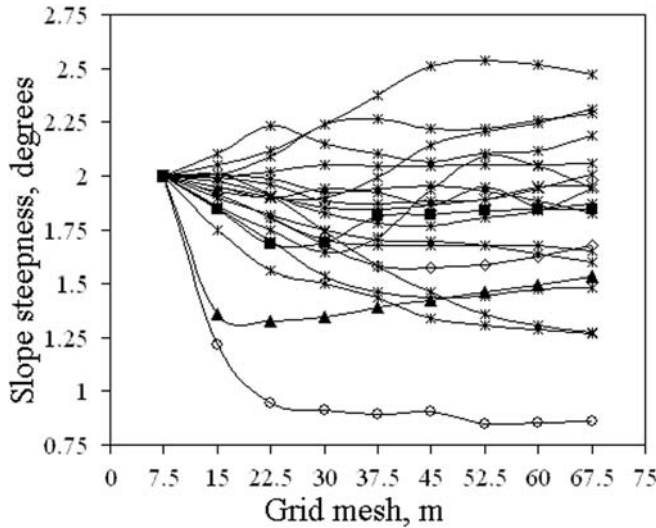


FIG. 14 - Dependence of slope steepness  $GA$  on grid mesh  $w$  for 20 points with values of  $GA$  approximately  $2^\circ$  at  $w = 7.5$  m.

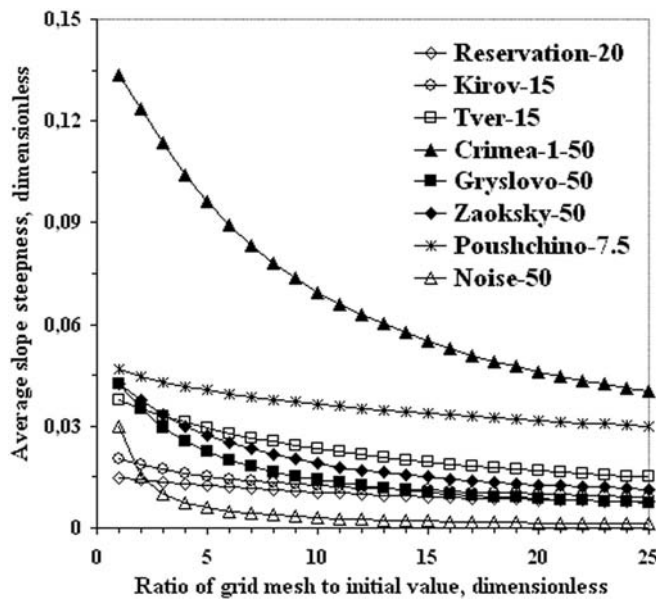


FIG. 15 - Dependence of average slope steepness  $G$  (dimensionless) on grid mesh for seven terrains and one model surface. Initial grid mesh (in meters) is indicated after abbreviation of each terrain.

as  $w$  increases, the logarithm of average slope steepness as a function of  $w$  in this case is a straight line that has negative slope (Shary & alii, 2002a).

This consideration shows that the average  $G$  of a noisy surface with a horizontal trend multiplied by grid mesh  $w$  should not depend on grid mesh, that is, it is a scale-free variable. This is shown by plots of  $w \cdot G_{AVER}$  against  $w$  of

fig. 16 for a set of territories, and also for some model noisy surfaces. We have multiplied  $G_{AVER}$  by  $w$  to make «Noise-50» a horizontal line.

As expected, noisy surfaces with non-horizontal trend (inclined plane «Noise-50, incl.» or cylinder with horizontal axis «Noise-50, cyl.») result in increase of curve slope as  $w$  grows, close to what is observed for real terrains. As  $w \rightarrow \infty$  for all observed terrains  $w \cdot G_{AVER}$  infinitely grows (fig. 16), while  $G_{AVER}$  monotonically decreases (fig. 15). That is, average slope steepness is proportional to  $1/w^a$  for real territories, where  $a$  lies between 0 and 1. Consequently, the morphometric characteristic  $G_{AVER} \cdot (w/w_0)^a$  does not depend on scale for these territories; here  $w_0$  is initial grid mesh for given terrain. A value of  $a$  may be chosen for the territories analysed equal to 0.21 that gives the weakest dependence of  $G_{AVER} \cdot (w/w_0)^a$  on grid mesh shown in fig. 17, as determined using the criterion of smallest (for the ten terrains) change in  $G_{AVER} \cdot w^a$ .

Note that average slope steepness is not a MV, the average value is an integral (sum) of values across a matrix, and therefore  $G_{AVER}$  is less scale-specific than slope steepness at a point. The general decline of slope steepness as grid mesh grows results, for example, that at  $w=2.25$  km the slope steepness in any point of the Moscow region (Russia) does not exceed  $1.4^\circ$ .

In contrast to differential MVs of classes A and C, integro-differential and integral MVs of class B may in some situations have clear limit values as  $w \rightarrow 0$ . For example,  $MCA$  on a thalweg becomes essentially an integral MV, because it is equal here to the area of up-slope part of basin. This means that  $MCA$  has a limit value on a thalweg as  $w \rightarrow 0$ . At the same time,  $MCA$  reaches its largest value on a map boundary so, this limit does exist, in part, for maximal value of  $MCA$  on a map (an exception be where a thalweg branches near map boundary), fig. 18.

Shary & alii (2002a) have provided also an example of the dependence of average depression depth on grid mesh, and have shown a limit value as  $w \rightarrow 0$  for this case also. So, regional MVs may have precise values, that is, a limit value as  $w \rightarrow 0$ , and be scale-free in this sense.

## LANDFORM CLASSIFICATIONS

One of first surface form classifications was suggested by Gauss (1827), fig. 19.

Gauss restricted his study by currently known in differential geometry short variant of this classification (by sign of  $K$ ), but he indicated the opportunity of the variant given here for some (orientable) surfaces. The land surface is one such surface that always has two sides, internal and external. Gaussian form types refer to class C, while Troeh's form types (fig. 4) refer to class A.

In general, Troeh's and Gauss's classifications are constructed following a similar principles of concave, convex and concave-convex forms. Nevertheless, Gaussian concave-convex form types (saddles) do not coincide with

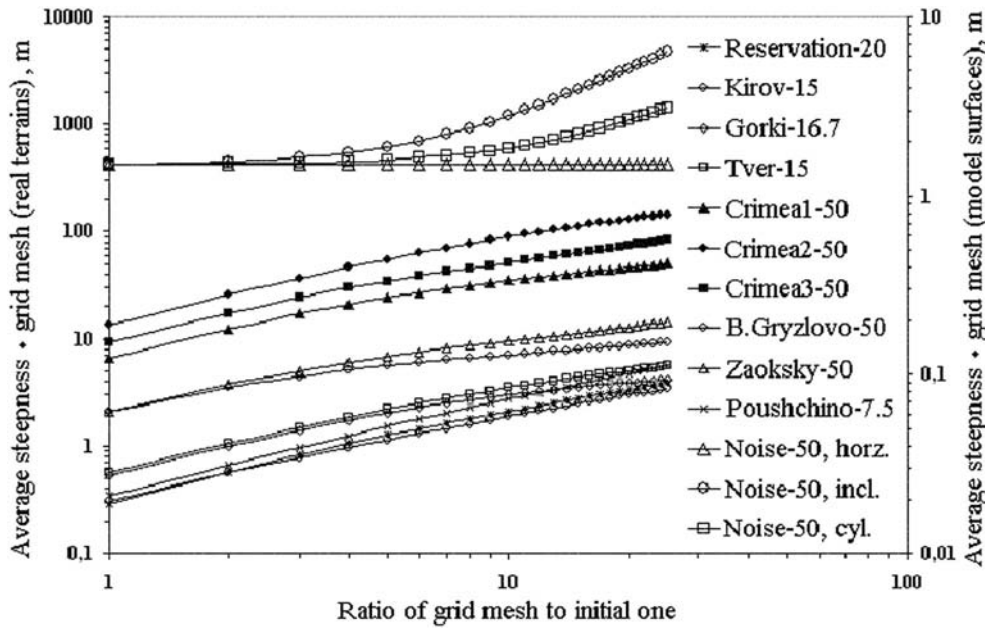


FIG. 16 - Dependence of  $G_{AVER} \cdot w$  on ratio of grid mesh  $w$  to initial value of grid mesh. Note that the curve «Noise-50, horz.» of noisy surface with a horizontal trend is a horizontal line.

Troeh's ones, because they ignore gravity, and consequently, the of slope profiles.

Shary (1995) has suggested a more general and flexible classification by curvature signs that includes Gauss's and Troeh's form types as partial cases. He has proven (*ibid*, theorem 2) that in spite of only three curvatures of (1) – (12) being independent, to define signs («→», 0, and «+»)

of all the 12 curvatures, one should use signs of 5 curvatures. He has proven also that not all areas are permitted in an abstract space HEM of the three independent curvatures, fig. 20.

In other words, a point in HEM-space that corresponds to any matrix element may appear only in permitted sectors of that space. Permitted areas are defined by

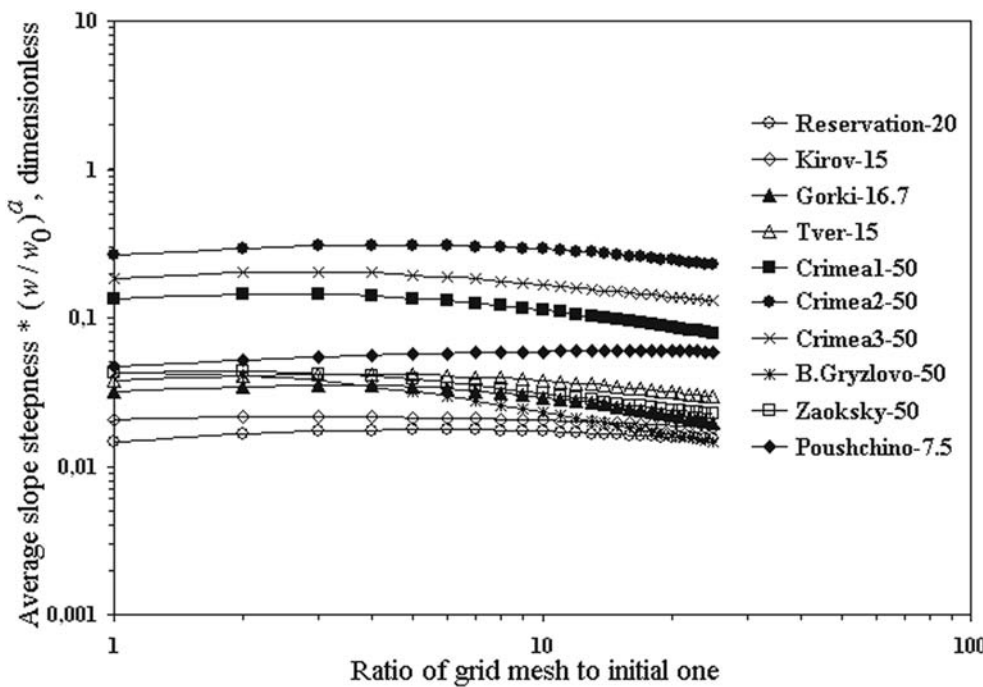


FIG. 17 - Dependence of  $G_{AVER} \cdot (w/w_0)^a$  on  $w/w_0$  at  $a=0.21$ .

FIG. 18 - Independence of maximal value of catchment area  $MCA$  on grid mesh for a part of southern Germany. This contrasts with the dependence on grid mesh of average slope steepness for the same terrain. SRTM data, equal-area Behrgman projection.  $MCA$  in Behrgman projection is calculated correctly (because areas are not distorted), but this projection might result in some distortions in average slope steepness; nevertheless, the latter does influence to the general dependence, as seen in fig. 15, where all result refer to Gauss-Krüger projection that correctly reflect distances.

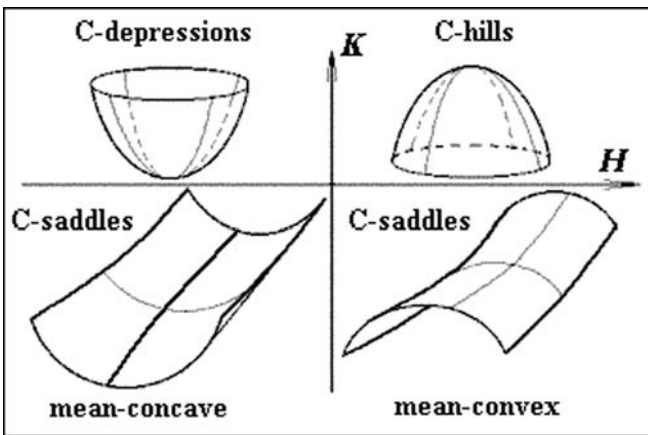
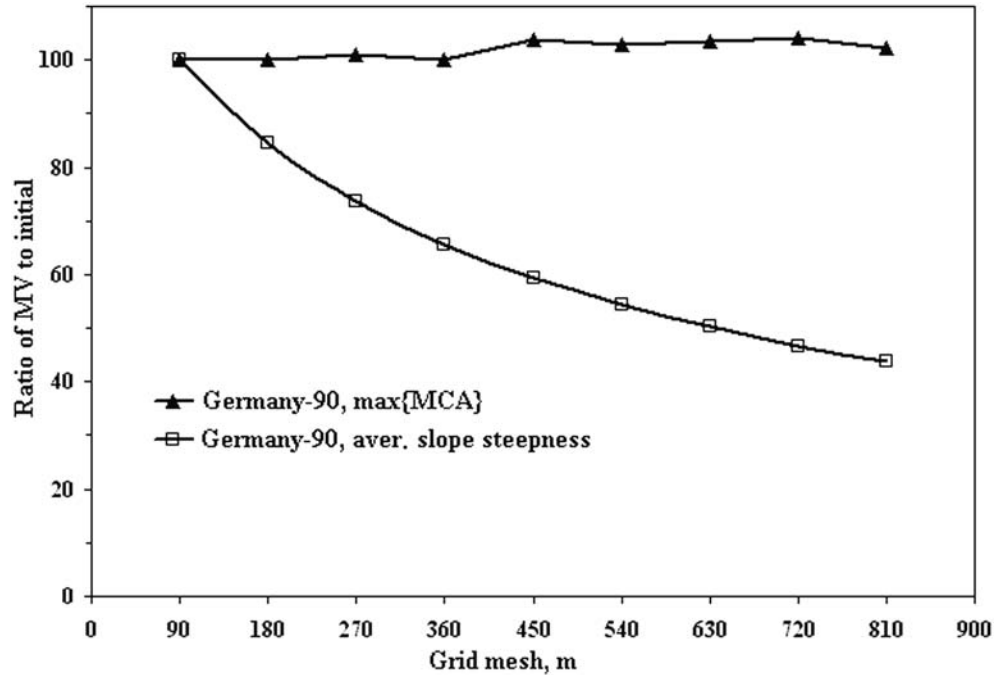


FIG. 19 - Gaussian surface form classification based on signs of total Gaussian curvature  $K$  and mean curvature  $H$ .

the two inequalities:  $M \geq 0$  and  $|E| \leq M$  (Shary, 1995). Gauss's and Troeh's classifications are related to HEM-space as shown in fig. 21.

A unique combination of signs of curvatures  $K$ ,  $H$ ,  $kv$ ,  $kb$ , and  $E$  corresponds to each permitted sector of HEM-space, thus giving Shary's land form classification onto 12 main land form types. Form types from Gauss and Troeh appear as compounds of Shary's, for example, Troeh's relative accumulation zones are composed of Shary's form types 1, 2, 7, and 8 (see fig. 21). fig. 22

shows how Troeh's relative accumulation zones are split into these form types.

In general, Shary's land form classification is shown in fig. 23. Its advantage consists in that it sub-divides land

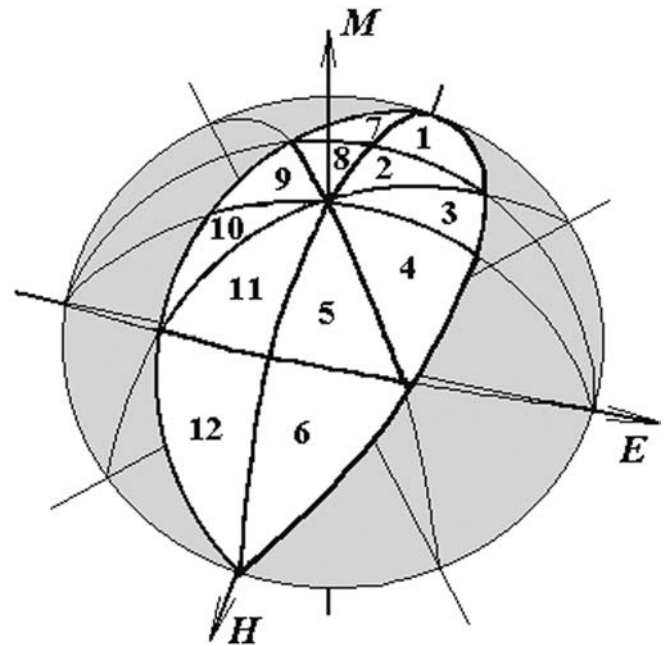


FIG. 20 - A sphere in HEM-space and 12 permitted sectors in it (shown by white). Not available portions of HEM-space are shown by gray.

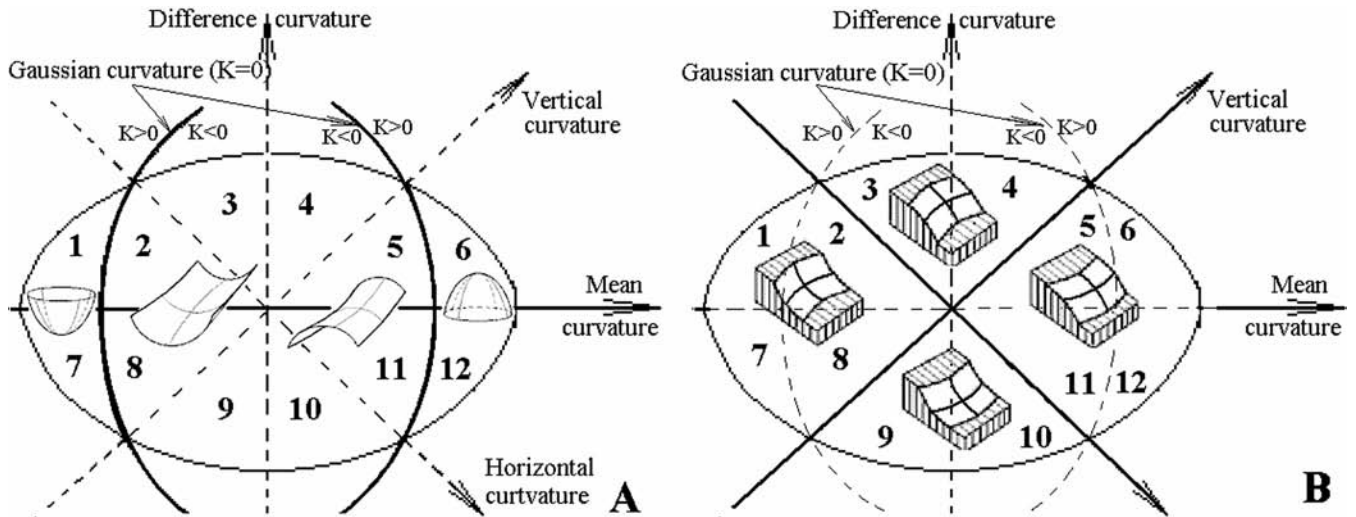


FIG. 21 - The relation of Gauss's and Troeh's land form types to HEM-space. A projection of this space onto plane  $M=0$  is shown. The sector numbers correspond to those in fig. 20.

forms onto more flexible «elementary» forms, thus allowing to construction of partial local classifications. Buivydaitė & Mozgeris (2004) have shown that Pearson's statistical contingency coefficients between Shary's form types and soil typological units is higher (at grid meshes 5 to 30 meters) than that for Gauss's or Troeh's classifications taken separately.

A simple general principle of classifying land form onto concave, convex and saddle parts can be realized also in class B, in a precise variant. We'll use a letter prefix that gives the class in which the form type is defined: C-depres-

sions (Gaussian), B-depressions (that are able to hold water), and so on. The boundary of a B-hill is the largest closed contour line that surrounds that hill on a map of a given extent. This contour line depends on map boundaries, unless we consider some naturally defined terrain portion, such as a continent or an island. This falls to a hierarchical concept of B-hills. Each larger B-hill is composed of smaller ones. When a whole continent is considered, a first continental level of a natural hierarchy of B-hills is defined (fig. 13). Similarly, the boundary of a B-depression is the largest closed contour line that surrounds it (as in fig. 1).

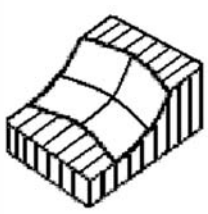
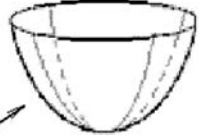
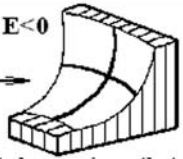
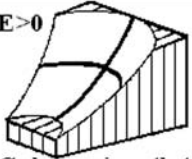
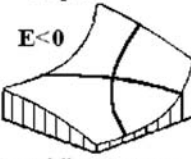
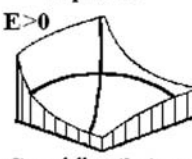
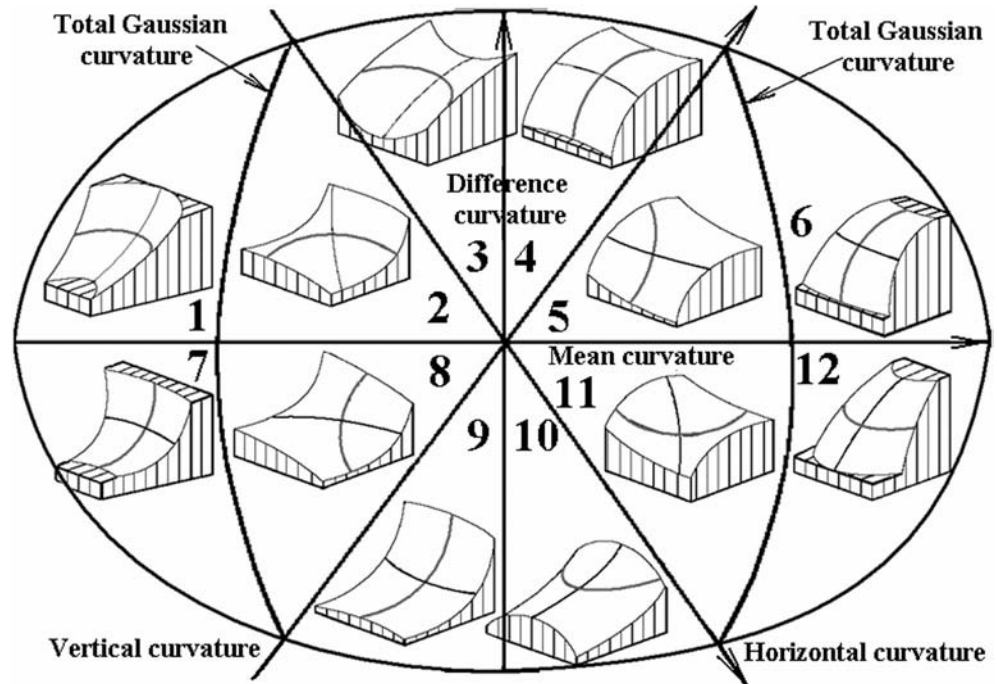
Troeh's land form types	Gaussian land form types	Elementary land forms	
$kh < 0, kv < 0$  Relative accumulation zones	$K > 0, H < 0$  C-depressions	$E < 0$  C-depressions that are more concave in profile than in plan	$E > 0$  C-depressions that are more concave in plan than in profile
	$K < 0, H < 0$  C-saddles mean-concave	$E < 0$  C-saddles that are more concave in profile than in plan	$E > 0$  C-saddles that are more concave in than in plan profile

FIG. 22 - Splitting of Troeh's relative accumulation zones onto the 4 Shary's form types.

FIG. 23 - Shary's land form classification.



Boundaries of B-hills and B-depressions cannot intersect. In a more strict sense, taking into account a possibility of contour lines intersections (Sard, 1942), there are no points that belong both to a B-hill and to a B-depression. Indeed, boundaries of B-hills or B-depressions, which are two different contour lines, should have a mutual point of their intersection where elevation would have two values, which is impossible in accordance to the topological restriction introduced above. Consequently, B-hills and B-depressions cannot intersect by their boundaries, although one may appear inside another. One can, however, include then other. An example would be one island in a lake (B-hill inside a B-depression) or a mountain lake (B-depression inside a B-hill). It seems to be natural to term the land surface space between B-hills and B-depressions as B-saddles, concave-convex surfaces of class B.

So, B-hills, B-depressions, and B-saddles sub-divide any terrain onto three non-overlapping types of regional forms with precisely defined boundaries. It is easy to calculate volume, area and other characteristics of any B-hill or B-depression (and these attributes are precise when sufficiently detailed maps are used, that is, sufficiently small grid meshes), but B-saddles have no volumes.

#### LOCAL LAND FORM PREDICTABILITY

Shary (1995) supposed that the area of any land form described by curvature signs may be predicted, in a statistical sense. This statistical hypothesis of Shary does not re-

fer to land form patterns, it refers only to areas. He has provided concrete values of area percentages, using the fact that each sector inside the HEM-sphere (fig. 20) has the same volume and from the suggestion that «clouds» of points, which correspond to matrix elements in this sphere, contain the same number of points inside any permitted sector. Therefore, each of Shary's main land form type would occupy 1/12 of any terrain. This fraction (probability) is easy to determine also for any form type of Gauss's or Troeh's classifications, from which that form type is composed, see fig. 21. For example, Gaussian C-depression is composed of two Shary's main land form types (1 and 7), and the probability is equal to 1/6; this probability equals 1/3 for the four Shary's form types which are mean-concave Gaussian C-saddles, that is, it is two times greater. Two thirds of land surface is composed of Gaussian saddles.

This hypothesis was checked experimentally using large data arrays (Sharaya & Shary, 2003) – 33 million matrix elements, jointly occupying 46,000 km<sup>2</sup>, – and was generally confirmed. For Gauss's and Troeh's forms it was true with an error not exceeding 25%, fig. 24.

Terrain specifics were with described only relatively small deviation from predicted values, fig. 25.

The 17 terrains refer to different countries and continents and vary from floodplains (low relief) to mountains (high relief). Most of DEMs for them were obtained using topographic maps. The reason why concave Troeh's form types dominate in mountainous terrains (as compared with gently sloping ones) consists in that denudation processes

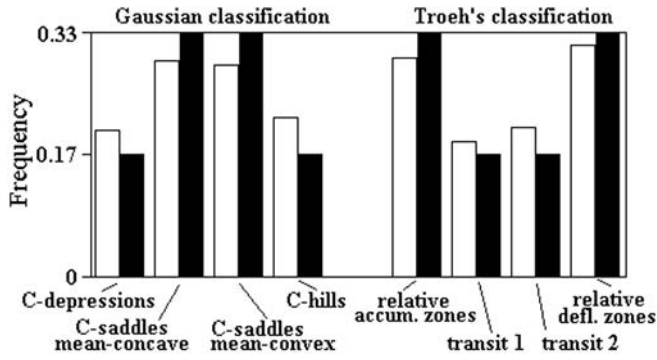


FIG. 24 - Comparison of observed (white) and predicted (black) frequencies of land form types of Gauss's and Troeh's classifications (12.8 millions of elements, grid mesh 30m, southern part of Washington State /USA/, SRTM data; this example is a part of the general research where 33 million of matrix were used).

tend to fulfill concave land forms by dry materials at geological times. Clearly, proportions of convex spurs and convex terraces diminish as relief increases.

No statistical predictability was observed for regional land form types. For example, the ratio of summary volumes of B-hills to that of B-depressions was 0.6 for Bavaria (Germany) with its deep lakes, was 10 for the gently sloping southern portion of Moscow region (Russia), and 10000 for mountainous central part of Hawaii

island (USA). Note volcanic origin of Hawaii island with its large mountain (4.2 km) and deeps depressions (120 m) at mountain's footslope not filled by fluvial processes or by water.

Evans (1980) has experimentally revealed a stable positive correlation between horizontal and vertical curvatures that was shown by this author for 60 terrains (Evans & Cox, 1999). We term this positive correlation the «Evans' phenomenon»; its origin was not clear for a long time.

The Evans' phenomenon is a consequence of Shary's statistical hypothesis, fig. 26.

Logarithmic transformation permits visual sub-division of the cloud of points of the scatter-plot at the plane ( $kb, kv$ ) into 4 parts; the number of points of relative accumulation and deflection zones (quadrants I and III in fig. 26), in accordance with Shary's statistical hypothesis, should be 2 times greater than that of transit zones (quadrants II and IV), thus resulting in the positive correlation between  $kv$  and  $kb$  that constitutes the Evans' phenomenon.

Note that land form types, for which at least one curvature is zero, are extremely rare; as a rule, they are related to artifacts in elevation matrices represented by horizontal plane areas that are due to elevation rounding (Sharaya & Shary, 2003). Shary (1995) has described 34 types of rare surface forms. Examples of rare (uncommon) forms are shown in fig. 27.

The statistical predictability of local land forms is a consequence of the non-smooth nature of the land surface. The latter may be considered as composed of «noisy» and

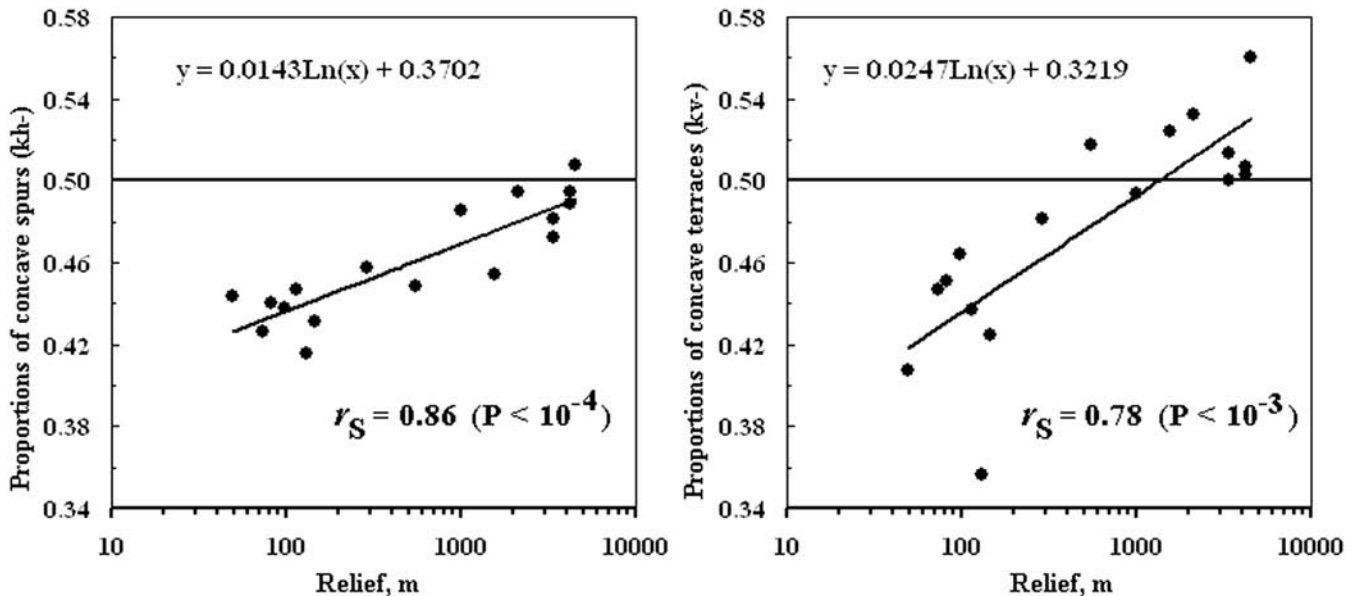


FIG. 25 - The dependence of proportions of Aandahl's concave spurs (negative  $kb$ ) and Aandahl's concave terraces (negative  $kv$ ) on relief (i.e., on the difference between maximal and minimal elevations) that characterized 17 terrains as mountainous or gently sloping (Sharaya & Shary, 2003). The horizontal lines refer to the predicted values.

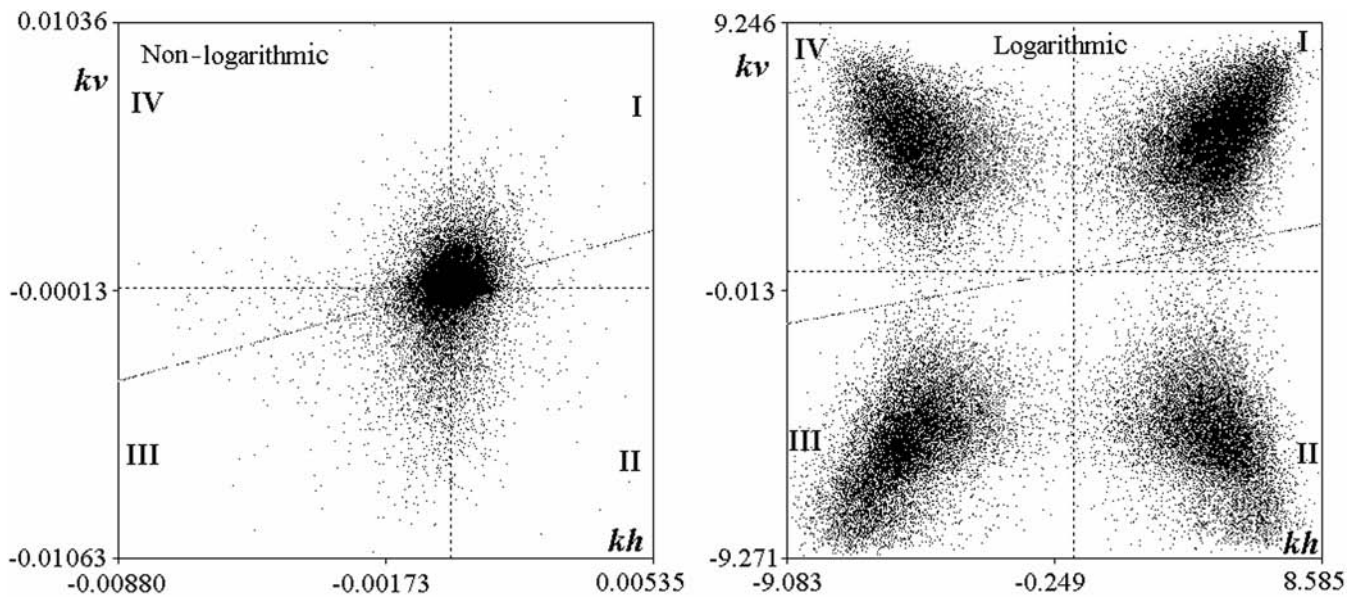


FIG. 26 - Scatter-plots of experimental points in coordinates of horizontal and vertical curvatures calculated for the same terrain as in fig. 3. Left - not logarithmic, right - logarithmic, using formula (1) by Shary & alii (2002a). Dashed line shows a linear trend.

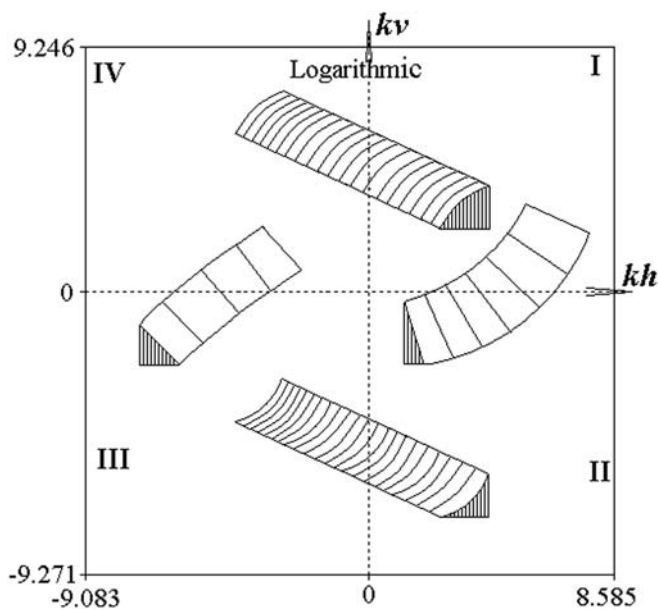


FIG. 27 - Rare forms types. Those at the axis  $kv$  have absolutely straight contour lines, those at the axis  $kh$  have absolutely straight slope profile. Absolutely plane surface (not shown) corresponds to co-ordinates origin ( $kv=kb=0$ ).

deterministic components (Tomer & Anderson, 1995); differentiation strengthens the noisy component, making properties of a curvature surface close to properties of quasi-stochastic surfaces, fig. 28.

This strengthening of the «noisy» component of non-smooth land surface by high-order derivatives creates the statistical predictability of land forms that are described by curvatures. The quasi-stochastic nature of curvature surface (fig. 28, bottom) results in a quasi-stochastic distribution of areas occupied by each land form type defined by curvature signs, that is, to the statistical predictability of these areas.

#### AN EXPERIMENTAL CHECK OF FLOW BRANCHING DURING OIL SPILLS

Freeman (1991) has suggested modification of MCA calculation in an algorithm after Martz & de Jong (1988), arguing this by weaker grid direction emphasizing when multiple flow-line branching is applied. The latter was not taken into account in the original algorithm (Martz & de Jong, 1988). Is the need for this modification physically substantiated, or does it just give more aesthetic map images of catchment area? Similarly, is taking account of multiple flow branching in oil spill analyses necessary, or does it only add deviations to the real pattern?

The results of an experimental check of an oil spill are shown in fig. 29, the process was fixed in a sequence of shots using video-camera.

This experiment, carried out jointly with the Center for Extreme Situations Research (Moscow, Russia), has confirmed the reality of multiple oil flow branching during oil spills. Oil flows branched on each out-of-scale hillock, with a confluence behind it. Such out-of-scale hillocks are

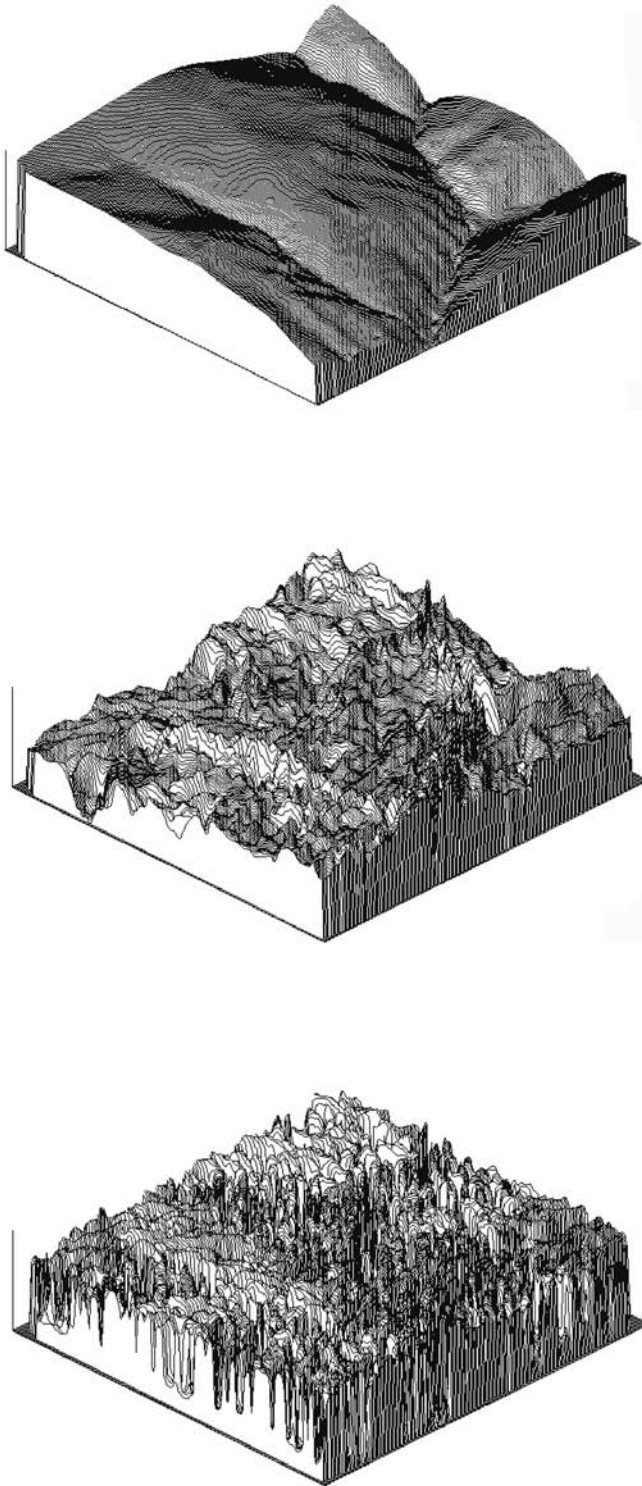


FIG. 28 - Three-dimensional view of elevation surface (top), of slope steepness surface (center), and of vertical curvature surface (bottom, of  $k_v$  logarithm) for the same terrain. It is seen that surfaces became closer to «noisy» ones as the order of derivatives increases (top to bottom).

numerous due to non-smooth nature of land surface, so that multiple flow-line branching and confluence is a physical reality. The same conclusion refers to catchment area *MCA* that is precisely a superposition of maximal distribution areas from each matrix element, with liquid quantity numerically equal to matrix element area (i.e., to squared grid mesh). Indeed, maximal distribution area is calculated using the same algorithm as *MCA*, with the difference that flows originate only from one pixel, and the liquid quantity is given instead of pixel area.

## DISCUSSION

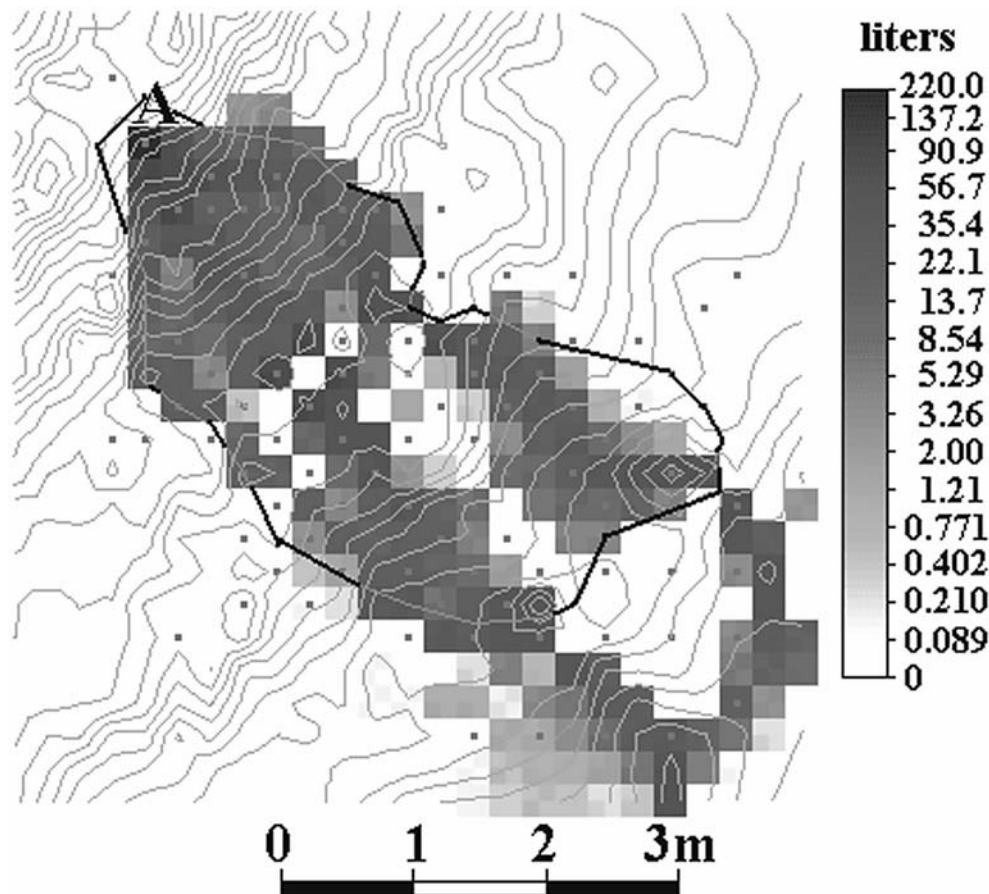
The non-smooth nature of the land surface results in morphometric variables (MVs) being clearly sub-divided into scale-free and scale-specific ones. For example, curvatures are scale-specific MVs. One consequence is that land form classifications based on their signs appear essentially predictable, in a statistical sense, and Evans' phenomenon of a stable positive correlation between horizontal and vertical curvatures appears common for almost any terrain. At the same time, it appears possible for average value of slope steepness to construct such characteristics that demonstrate weak dependence on map scale, providing an opportunity to use such MVs in future as scale-free analogs of average values of some scale-free MVs.

On the other hand, some regional MVs demonstrate limit values as grid mesh tends to zero, that is, in a large-scale limit. This concept of precision coincides with that known in geodesy for elevations. Although the theory of local MVs is in fact close to completeness – Shary (1995) has proven the completeness of the system of 12 curvatures, – the theory of regional MVs needs further development, because few basic MVs are known in class B, and class D is currently empty. For example, important concepts of D-depressions and D-hills that describe memory in geosystems remain not developed (Mitusov & Shary, 2001; Shary & alii, 2002a). Ideas of some new MVs were suggested by Shary & alii (2002a). It seems desirable to develop MVs of classes B and D further, because such MVs provide a basis for comparable studies at different scales.

Larger number of MVs may be found, for example, in Wilson & Gallant (2000), although they are mostly various (often non-strictly defined) combinations of the basic MVs described herein; there are no arguments to consider the question of their scale dependence.

The availability of new planetary high-resolution elevation matrices, such as the SRTM of 90-m resolution, may potentially stimulate the development of new MVs of classes B and D. The authors are always open for exchange of ideas in this area.

FIG. 29 - Experimental study of oil spills. 220 liters of wet oil were placed at point A. Lines are contour lines; oil concentration was measured at 102 points; the polygon shows a trace of surface waste, colors show distribution area. Grid mesh is 0.25 m.



#### LITERATURE CITED

- AANDAHL A.R. (1948) - *The characterization of slope positions and their influence on the total nitrogen content of a few virgin soils of Western Iowa*. Soil Science Society of America Proceedings, 13, 449-454.
- BEVEN K.J. & KIRKBY M.J. (1979) - *A physically based, variable contributing area model of basin hydrology*. Hydrological Sciences Bulletin, 24, 43-69.
- BEVEN K.J. & WOOD E.F. (1983) - *Catchment geomorphology and the dynamics of runoff contributing areas*. Journal of Hydrology, 65, 139-158.
- BEVEN K.J. (1987) - *Towards the use of catchment geomorphology in flood frequency predictions*. Earth Surface Processes and Landforms, 12, 69-82.
- BUIVYDAITE V.V. & MOZGERIS G. (2004) - *Digital land surface analysis: on possibilities of applications in soil survey*. Eurosoil, 2004. 14 p. Available as .PDF file at the website [http://kuk.uni-freiburg.de/hosted/eurosoil2004/full\\_papers/id995\\_Buivydaite\\_full.pdf](http://kuk.uni-freiburg.de/hosted/eurosoil2004/full_papers/id995_Buivydaite_full.pdf).
- COSTA-CABRAL M.C. & BURGESS S.J. (1994) - *Digital elevation model networks (DEMON): A model of flow over hillslopes for computation of contributing and dispersal areas*. Water Resources Research, 30, 1681-1692.
- EVANS I.S. (1972) - *General geomorphometry, derivatives of altitude, and descriptive statistics*. In: Chorley, R.J. (ed.), «Spatial Analysis in Geomorphology». Methuen & Co., Ltd., London, Chap. 2, pp. 17-90.
- EVANS I.S. (1975) - *The effect of resolution on gradients calculated from an altitude matrix*. Report 3 on Grant DA-ERO-591-73-G0040, 'Statistical characterization of altitude matrices by computer' (Appendix: Stationarity). Department of Geography, University of Durham, England, 24 pp.
- EVANS I.S. (1980) - *An integrated system of terrain analysis and slope mapping*. Zeitschrift für Geomorphologie N.F., Suppl.-Bd. 36, 274-295.
- EVANS I.S. & COX N.J. (1999) - *Relations between land surface properties: altitude, slope and curvature*. In: Hergarten S., Neugebauer H.J. (eds.). «Process Modelling and Landform Evolution». Berlin, etc., Springer, pp. 13-45.
- FLANAGAN D.C., RENSCHLER C.S. & COCHRANE T.A. (2000) - *Application of the WEPP model with digital geographic information. Problems, Prospects and Research Needs. 4th International Conference on Integrating GIS and Environmental Modeling (GIS/EM4)*. Banff, Alberta, Canada, September 2 - 8, 2000, GIS/EM4 No. 149. Available at the website <http://www.colorado.edu/research/cires/banff/pubpapers/149/>
- GAUSS K.F. (1827) - *Disquisitiones generales circa area superficies curvas*. Göttingen gel. Anz., No. 177, pp. 1761-1768 (in Latin).
- JENSON S.K. & DOMINGUE J.O. (1988) - *Extracting topographic structure from digital elevation data for geographic information system analysis*. Photogrammetric Engineering and Remote Sensing, 54, 1577-1580.
- KLEMEŠ V. (1983) - *Conceptualization and scale in hydrology*. Journal of Hydrology, 65, 1-23.
- KOENDERINK J.J. & VAN DOORN A.J. (1994) - *Two-plus-one-dimensional differential geometry*. Pattern Recognition Letters, 15, 439-443.

- KRCHO J. (1973) - *Morphometric analysis of relief on the basis of geometric aspect of field theory*. Acta Geographica Universitatis Comenianae, Geographico-Physica, 1, 7-233.
- KRCHO J. (1983) - *Teoretická koncepcia a interdisciplinárne aplikácie komplexného digitálneho modelu reliéfu pri modelovaní dvojdimenzionálnych poli*. Geografický časopis, 35, 265-291 (in Slovak).
- MANDELBROT B. (1967) - *How long is the coast of Britain? Statistical self-similarity and fractional dimension*. Science, 156, 636-638.
- MARK D.M. (1979) - *Topology of ridge patterns: Randomness and constraints*. Geological Society of America Bulletin, Part I, 90, 164-172.
- MARTZ L.W. & DE JONG E. (1988) - *CATCH: a Fortran program for measuring catchment area from digital elevation models*. Computers and Geosciences, 14, 627-640.
- MARTZ L.W. & DE JONG E. (1990) - *Natural radionuclides in the soils of a small agricultural basin in the Canadian Prairies and their association with topography, soil properties and erosion*. Catena, 17, 85-96.
- MCKENZIE N.J. & RYAN P.J. (1999) - *Spatial prediction of soil properties using environmental correlation*. Geoderma, 89, 67-94.
- MITAS L., MITASOVA H., BROWN W.M. & ASTLEY M. (1996) - *Interacting fields approach for evolving spatial phenomena: application to erosion simulation for optimized land use*. Proceeding of the III International Conference on Integration of Environmental Modeling and GIS (Santa Fe, NM, USA). National Center for Geographic Information and Analysis: Santa Barbara CA. Available at the website: <http://skagit.meas.ncsu.edu/~helena/gmslab/reports/CerlErosionTutorial/denix/Advanced/InteractingFields/lfields/index.html>
- MITAS L., BROWN W.M. & MITASOVA H. (1997) - *Role of dynamic cartography in simulations of landscape processes based on multi-variate fields*. Computers and Geosciences, 23, 437-446.
- MITAS L. & MITASOVA H. (1998) - *Distributed soil erosion simulation for effective erosion prevention*. Water Resources Research, 34, 505-516.
- MITASOVA H. & HOFIERKA J. (1993) - *Interpolation by regularized spline with tension. II. Application to terrain modeling and surface geometry analysis*. Mathematical Geology, 25, 657-669.
- MITASOVA H., HOFIERKA J., ZLOCHA M. & IVERSON R.L. (1996) - *Modeling topographic potential for erosion and deposition using GIS*. International Journal of Geographical Information Science, 10, 629-641.
- MITASOVA H., MITAS L., BROWN W.M. & JOHNSTON D. (1997) - *GIS tools for erosion/deposition modeling and multidimensional visualization. Part IV: Process based erosion simulation for spatially complex conditions and its applications to installations. Part V: Impact of transport capacity and terrain structures on erosion simulations*. Report for USA CERL. Urbana-Champaign: University of Illinois, 1997. 30p. Available at the website: <http://skagit.meas.ncsu.edu/~helena/gmslab/reports/CerlErosionTutorial/denix/Advanced/ErosionRep97/rep97.html>
- MITUSOV A.V. & SHARY P.A. (2001) - *Application of quantitative land surface analysis methods to soil water content spatial variability studies*. In: K.-P. Seiler, S. Wöhllich (eds.). *New Approaches Characterizing Groundwater Flow*. Proceedings of the XXXI International Association of Hydrogeologists Congress, Munich, Germany, September 10-14, 2001. Swets and Zeitlinger Lisse / Abingdon / Exton / Tokyo: A.A. Balkema Publishers, 2001, Vol. 2, pp. 757-761.
- MONTGOMERY D.R. (1994) - *Road surface drainage, channel initiation and slope instability*. Water Resources Research, 30, 1925-1932.
- PENNOCK D.J., ZEBARTH B.J. & DE JONG E. (1987) - *Landform classification and soil distribution in hummocky terrain, Saskatchewan, Canada*. Geoderma, 40, 297-315.
- PHILLIPS J.D. (1988) - *The role of spatial scale in geomorphic systems*. Geographical Analysis, 20, 308-317.
- RAFAELLI S.G., MONTGOMERY D.R. & GREENBERG H.M. (2001) - *A comparison of thematic mapping of erosional intensity to GIS-driven process models in an Andean drainage basin*. Journal of Hydrology, 244, 33-42.
- RODHE A., NYBERG L. & BISHOP K. (1996) - *Transit times for water in a small till catchment from a step shift in the oxygen 18 content of the water input*. Water Resources Research, 32, 3497-3511.
- RYAN P.J., MCKENZIE N.J., O'CONNELL D., LOUGHHEAD A.N., LEPPERT P.M., JACKUIER D. & ASHTON L. (2000) - *Integrating forest soils information across scales: spatial prediction of soil properties under Australian forests*. Forest Ecology and Management, 138, 139-157.
- SARD A. (1942) - *The measure of the critical values of differentiable maps*. Bulletin of American Mathematical Society, 48, 883-890.
- SCHMIDT J., EVANS I.S. & BRINKMANN J. (2003) - *Comparison of polynomial models for land surface curvature calculation*. International Journal of Geographical Information Science, 17, 797-814.
- SHARAYA L.S. & SHARY P.A. (2003) - *Use of morphometric statistics to describe internal geometry of gently sloping and mountainous territories*. Izvestiya Samarskogo nauchnogo centra RAS, 5, 278-286. (In Russian).
- SHARY P.A. & STEPANOV I.N. (1991) - *On the second derivative method in geology*. Doklady of the USSR Academy of Sciences 319, 456-460. (In Russian).
- SHARY P.A. (1995) - *Land surface in gravity points classification by a complete system of curvatures*. Mathematical Geology, 27, 373-390.
- SHARY P.A. (2001) - *Analytical GIS Eco, help system and description*. Available at the websites <http://members.fortunecity.com/eco4/giseco/> and [http://members.fortunecity.com/eco4/research\\_shary/](http://members.fortunecity.com/eco4/research_shary/)
- SHARY P.A., SHARAYA L.S. & MITUSOV A.V. (2002a) - *Fundamental quantitative methods of land surface analysis*. Geoderma, 107, 1-32.
- SHARY P.A., RUKHOVICH O.V., SHARAYA L.S. & MITUSOV A.V. (2002b) - *Soils and topography: accumulation zones and non-local approaches*. Transactions of 17-th World Congress of Soil Science, «Soil Science: Confronting New Realities in the 21-st Century», held in Bangkok, Thailand, August 14-21, 2002. Volume IV. Symposium 48: «Development in soil data processing», Paper No.2310. Full paper: pp. 2310-1 - 2310-11, Abstract: p. 1493.
- SPEIGHT J.G. (1968) - *Parametric description of land form*. Stewart G.A. (ed.), *Land Evaluation*. London: Macmillan, p. 239-250.
- SPEIGHT J.G. (1974) - *A parametric approach to landform regions*. *Progress in Geomorphology*. Institute of British Geographers special publ. No.7. Oxford: Alden & Mowbray Ltd at the Alden Press, 1974, pp. 213-230.
- STRAHLER A.N. (1952) - *Hypsometric (area-altitude) analysis of erosional topography*. Bulletin of the Geological Society of America, 63, 1117-1141.
- TOMER M.D. & ANDERSON J.L. (1995) - *Variation of soil water storage across a sand plain hillslope*. Soil Science Society of America Journal, 59, 1091-1100.
- WIGMOSTA M.S., VAIL L.W. & LETTENMAIER D.P. (1994) - *A distributed hydrology-vegetation model for complex terrain*. Water Resources Research, 30, 1665-1679.
- WILSON J.P. & GALLANT J.C. (eds.) (2000) - *Terrain Analysis: Principles and Applications*. New York: John Wiley & Sons Inc. 320 pp.
- YOUNG T. (1805) - *An essay on the cohesion of fluids*. Philosophical Transactions of the Royal Society of London, 95, 55-87.
- YOUNG M. (1978) - *Terrain analysis: program documentation*. Report 5 on Grant DA-ERO-591-73-G0040, 'Statistical characterization of altitude matrices by computer'. Department of Geography, University of Durham, England. 27 pp.
- ZEVENBERGEN L.W. & THORNE C.R. (1987) - *Quantitative analysis of land surface topography*. Earth Surface Processes and Landforms, 12, 47-56.

#### APPENDIX. THE MODIFIED EVANS-YOUNG ALGORITHM

The Evans-Young method consists in the following. The 2-nd order polynomial  $z = rx^2/2 + sxy + ty^2/2 + px + qy + z_0$  is fitted by the least squares method to the subgrid  $3 \times 3$ , with grid mesh  $w$  and elevations in nodes  $z_1, \dots, z_9$ . The locations and numbering of nodes are shown in fig. A1.

This gives the following formulae for coefficients  $p, q, r, s, t$  of the polynomial:

$$\begin{aligned} p &= (z_3+z_6+z_9-z_1-z_4-z_7)/6w, \\ q &= (z_1+z_2+z_3-z_7-z_8-z_9)/6w, \\ r &= [z_1+z_3+z_4+z_6+z_7+z_9-2(z_2+z_5+z_8)]/3w^2, \\ s &= (-z_1+z_3-z_7+z_9)/4w^2, \\ t &= [z_1+z_2+z_3+z_7+z_8+z_9-2(z_4+z_5+z_6)]/3w^2; \end{aligned}$$

see details on deduction of these formulae in Young (1978), reproduced in Pennock & alii (1987).

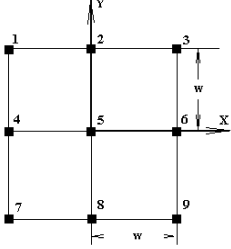


FIG. A1 - Locations and numbering of nodes in subgrid  $3 \times 3$ .

The coefficients  $p, q, r, s, t$  are partial derivatives of the polynomial at the central point of the subgrid that has coordinates  $x=y=0$ . Namely,  $p=\partial z/\partial x$ ;  $q=\partial z/\partial y$ ;  $r=\partial^2 z/\partial x^2$ ;  $s=\partial^2 z/\partial x \partial y$ ;  $t=\partial^2 z/\partial y^2$ . Now, using these values of partial derivatives, one may calculate for the central (5-th) point of the subgrid  $3 \times 3$  any local morphometric variables that

are expressed by first and second derivatives from elevations of the surface given by the equation  $z=z(x,y)$ . Then the subgrid  $3 \times 3$  is moved by its center to another element of the elevation matrix, and the procedure is repeated. Calculations are carried out for all but boundary matrix elements.

The modification of Evans-Young method consists in that before calculations by this method a parametric isotropic smoothing of the initial elevation matrix is performed. This smoothing is realized by replacing the elevation  $z_5$  in the central point (5-th, fig. A1) by a new value  $z_5'$ , that is linearly expressed through  $3 \times 3$  subgrid points elevations:

$$z_5' = a_1 z_1 + a_2 z_2 + a_3 z_3 + a_4 z_4 + a_5 z_5 + a_6 z_6 + a_7 z_7 + a_8 z_8 + a_9 z_9. \quad (1A)$$

There are 9 unknown weights,  $a_1, \dots, a_9$ , for the filter (1A). The first condition for their determination consists in that (A) *a plane piece of surface is transformed into a plane one*. An equation of a plane is  $z=ax+\beta y+z_5$ ; substituting into this formula the coordinate values  $x, y$  of subgrid nodes (fig. A1), one obtains

$$\begin{aligned} z_1' &= w(-\alpha+\beta)+z_5, & z_2' &= \beta w+z_5, & z_3' &= w(\alpha+\beta)+z_5, \\ z_4' &= -\alpha w+z_5, & z_5' &= z_5, & z_6' &= \alpha w+z_5, \\ z_7' &= w(-\alpha-\beta)+z_5, & z_8' &= -\beta w+z_5, & z_9' &= w(\alpha-\beta)+z_5; \end{aligned}$$

it follows from this for an arbitrary plane

$$z_5' = \alpha w(-a_1+a_3-a_4+a_6-a_7+a_9) + \beta w(a_1+a_2+a_3-a_7-a_8-a_9) + z_5 \sum a_i$$

The left part of this equation must be equal to  $z_5$ , because the filter does not change elevations for the plane:

$$(1-\sum a_i)z_5 = \alpha w(-a_1+a_3-a_4+a_6-a_7+a_9) + \beta w(a_1+a_2+a_3-a_7-a_8-a_9). \quad (2A)$$

Because  $a_1, \dots, a_9$  are numbers and the last equality should be valid for any  $\alpha, \beta, z_5$ , all the three parentheses in (2A) must be equal to zero. From here

$$a_1+a_2+a_3+a_4+a_5+a_6+a_7+a_8+a_9=1, \quad (3A)$$

$$a_3+a_6+a_9-a_1-a_4-a_7=0, \quad a_1+a_2+a_3-a_7-a_8-a_9=0. \quad (4A)$$

The next condition is that (B) *the filter is isotropic*. This means that all weights are dependent only from the distance between node and central point. One finds from here the equalities  $a_1=a_3=a_7=a_9$ ,  $a_2=a_4=a_6=a_8$ , from which equalities (4A) follow automatically; the equality (3A) takes now the form

$$a_5 = 1 - 4(a_1 + a_2). \quad (5A)$$

The filter (1A) is now  $z_5' = a_1(z_1+z_3+z_7+z_9) + a_2(z_2+z_4+z_6+z_8) + a_5 z_5$ ; substituting here  $a_5$  from (5A), one finds:

$$z_5' = a_1(z_1+z_3+z_7+z_9) + a_2(z_2+z_4+z_6+z_8) + [1-4(a_1+a_2)]z_5. \quad (6A)$$

So, the conditions (A) and (B) leave unknown the two weights of the filter (1A):  $a_1$  and  $a_2$ . One from them can be defined by the condition of (C) *linearity of weights decreasing with a distance from the central point*. Let us rewrite (6A) for this in the form

$$z_5' = k(z_1+z_3+z_7+z_9)/9 + s(z_2+z_4+z_6+z_8)/9 + [1-4(k+s)/9]z_5,$$

where the smoothing parameter  $s \in [0, 1]$ , and the condition (C) gives for  $k$  the expression

$$k = 1 - 2^{1/2}(1-s) \text{ for } s \in [1-2^{-1/2}, 1] \quad \text{and} \quad k = 0 \text{ for } s \in [0, 1-2^{-1/2}].$$

The remaining free parameter  $s$  determines extent of surface smoothing by the filter. An absence of smoothing ( $z_5' = z_5$ ) corresponds to the value  $s=0$ , non-weighted average  $z_5' = \sum z_i/9$  of the grid points corresponds to the value  $s=1$ . At  $s < 1-2^{-1/2} \approx 0.293$  the expression for  $z_5'$  is simplified, because of  $k=0$ :

$$z_5' = s(z_2+z_4+z_6+z_8)/9 + (1-4s/9)z_5.$$

It was empirically stated that  $s=1/5$  («weak» smoothing) gives good results for maps of curvatures for practically any terrain. For this value the last formula takes the form

$$z_5' = (z_2+z_4+4z_5+z_6+z_8)/45.$$

Smoothing of 9 points of the subgrid  $3 \times 3$  by this filter with subsequent use of the Evans-Young method to this smoothed subgrid results in the modified Evans-Young method.